Acta Cryst. (1958). **11**, 331

The Crystal Structures of Low-Temperature and High-Temperature Albites*

By R. B. Ferguson

Crystallographic Laboratory, Cavendish Laboratory, Cambridge, England, and Department of Geology, University of Manitoba, Winnipeg, Canada

R. J. Traill†

Department of Geological Sciences, Queen's University, Kingston, Ontario, Canada, and Department of Geology, University of Manitoba, Winnipeg, Canada

and W. H. Taylor

Crystallographic Laboratory, Cavendish Laboratory, Cambridge, England

(*Received* 8 *March* 1957)

Starting with the structure of (low) albite published by Taylor, Darbyshire & Strunz in 1934, the crystal structures of a low albite and of a high albite, both nearly pure $NaAlSi_3O_8$, have been refined by means of a series of F_o and (F_o-F_c) Fourier projections parallel to all three axes. The mean bond lengths within the four non-equivalent tetrahedra are in low albite, $1{\cdot}74_2$, $1{\cdot}59_0$, $1{\cdot}63_6$ and $1{\cdot}61_6$ Å, and in high albite $1{\cdot}65_2$, $1{\cdot}63_9$, $1{\cdot}64_2$ and $1{\cdot}64_7$ Å, with a standard deviation 0·02 Å. It is concluded that in low albite the first site $Si_1(0)$ contains nearly all the Al and that in high albite the Al and Si atoms are randomly distributed throughout the four tetrahedral sites. The dimorphism of soda felspar is thus due primarily to differences in the degree of Al–Si ordering.

Four features of the Na atom were noted: (1) In both albites the temperature factor of this atom is much greater than that implied in the *f* curve of Bragg & West. (2) The temperature factor is greater in high albite than in low. (3) In low albite this atom behaves as though it had an anisotropic thermal vibration with a maximum amplitude nearly along *y* equivalent to an atomic separation of ~ 0·1 Å. (4) In high albite the effect is similar but much more intense, equivalent to a separation of ~ 0·6 Å. A possible interpretation is that the Na atom occupies at random through the structures one or other of two positions, within the same large cavity, separated by ~ 0·1 Å or ~ 0·6 Å nearly along *y*. On this view, when the Al–Si atoms are disordered as in high albite the cavity available for Na is effectively larger than that atom can fill, whereas when the Al–Si atoms are largely ordered, as in low albite, the cavity is small enough to nearly enclose the Na atom.

On the assumption that maximum stability at room temperature corresponds to local balance of electrostatic charges throughout the structure, a detailed discussion of the two albites and of sanidine and intermediate microcline leads to a number of unexpected and important conclusions: (1) In low-temperature felspars the most stable structure is not necessarily, as is generally assumed, one in which the Al–Si atoms are completely ordered. (2) The most stable potassium felspar is not 'maximum' microcline but a monoclinic (*C*2/*m*) orthoclase with Al partially ordered into one half of the tetrahedra. (3) Intermediate microcline has an unstable charge distribution and all microclines lie outside the normal stability range of the potassium felspars, which runs from disordered sanidine to partially ordered orthoclase. (4) Most microclines probably form as the exsolution product of an alkali felspar which cooled from fairly high temperatures and which, at those high temperatures, contained a sufficient proportion of Na to confer partial ordering and the associated triclinic symmetry on the tetrahedral framework.

General introduction

Sodium felspar ($NaAlSi_3O_8$) may exist in one of two well established modifications. The ordinary low-temperature form, called variously low-temperature albite, low albite or simply albite, is widespread in acid plutonic rocks. The much rarer high-temperature form, called variously high-temperature albite, high albite, or analbite, has been reported from some acid lavas and may be produced synthetically by crystallizing a glass of albite composition or by heating the low-temperature modification for long periods. Of the possible names for the two forms we prefer low albite and high albite, which are already gaining wide acceptance.

The crystal structure of (low) albite was described

* Progress reports on this work were given at the Third Congress of the International Union of Crystallography in Paris, 1954 (*Acta Cryst.* (1954), **7**, 633) and at the Fourth Congress in Montreal, 1957 (*Acta Cryst.* (1957), **10**, 759).

† Present address: Geological Survey of Canada, Ottawa, Ontario, Canada.

by Taylor, Darbyshire & Strunz (1934) shortly after Taylor (1933) had established the structure of sanidine. In the later paper, the authors showed that all felspars have essentially the same structure and that the small structural difference between albite and sanidine is due to a slight collapse of the tetrahedral framework about the smaller alkali atom in albite. The symmetry is thus lowered from monoclinic to triclinic, and this early analysis showed that atoms in albite are shifted up to 0·3 Å from the positions of their counterparts in sanidine. The general structural features of the felspar minerals, including albite, are well known and need not be reviewed here.

Highly accurate structure analyses of the two modifications of albite were undertaken by the writers for several reasons. First, to try to distinguish between the Al and Si atoms (not differentiated in the early analysis) in order to determine whether the principal structural difference between the two forms is due to Al–Si order–disorder as Barth (1934) postulated for the potassium felspars, and as Cole, Sörum & Kennard (1949) and Bailey & Taylor (1955) have now proven for those felspars. Second, to determine any structural differences other than the presumed Al–Si order–disorder. And, third, to provide accurate structural data needed for the elucidation of the complex intermediate members of the two important series, the alkali (potassium–sodium) felspars and the plagioclase (sodium–calcium) felspars.

High albite has optical and crystallographic properties close to those of the low-temperature form. In particular, Laves & Chaisson (1950) have shown that the two modifications have very similar triclinic cell dimensions, the same cell content, and similar X-ray patterns, and have suggested that structural differences between the two forms are small. We have assumed that the structures of both modifications could be refined by starting with the parameters of low albite published in 1934. In this way we have derived accurate structures for a low albite and a high albite, both nearly pure $NaAlSi_3O_8$, by means of a series of two-dimensional F_o and (F_o-F_c) Fourier syntheses for each of the three principal projections. The principal structural difference between the two modifications is shown to be a largely ordered distribution of the Al and Si atoms in low albite and a random distribution in high albite. Other secondary structural differences have been revealed, particularly with reference to the sodium atom.

In this work we have used only two-dimensional Fourier syntheses, and certain atoms are not fully resolved in any of the three projections. Because of the great geological importance of the soda felspars, we plan to refine the structures of both modifications still further by three-dimensional methods which permit full resolution of all atoms. Much preparatory work has already been done, but because considerable time will be required to manipulate the measurements for several thousand reflexions, and because our present results appear to be fairly conclusive, we have thought it advisable to publish them now.

Parts I and II of the paper describe the analyses of the structures of low albite and high albite respectively. In Part III we discuss our results.

PART I. LOW ALBITE

By R. B. Ferguson

1. Experimental details

The specimen chosen for examination was No. 29 of a suite of plagioclase felspars given by R. C. Emmons to W. H. Taylor. Emmons and his colleagues at the University of Wisconsin have published (Emmons, 1953) detailed chemical and optical descriptions of these felspars as part of a broader geological investigation. The history of specimen No. 29 (Emmons, 1953, and private communication) is: collected by Waldemar T. Schaller from the Little Three Mine, Ramona, San Diego County, California, where it occurred in a cavity in an albitized pegmatite; listed

Table 1. *Chemical analyses and molecular compositions* of Ramona and Amelia albites*

(Emmons, 1953, p. 19)

	Ramona (Emmons No. 29)	Amelia (Emmons No. 31)
Analyst	R. E. Stevens	R. E. Stevens
SiO_2	68·05	68·17
Al_2O_3	19·73	19·62
Fe_2O_3	0·10	0·08
MgO	Trace	Trace
CaO	0·05	0·08
Na_2O	11·69	11·59
K_2O	0·18	0·28
H_2O^-	0·03	0·01
H_2O^+	0·10	0·11
TiO_2	0·01	0·01
Total	99·94	99·95
Or*	1·0	1·6
Ab	98·5	97·7
An	0·5	0·7

* Expressed as molecular percentages of $KAlSi_3O_8$, $NaAlSi_3O_8$, and $CaAl_2Si_2O_8$.

Table 2. *Optical data for Ramona albite and inverted Amelia albite*

	Ramona* (Emmons No. 29)	Amelia, inverted† (Emmons No. 31)
α	1·528	1·527
β	1·532	1·532
γ	1·538	1·534
$2V_\gamma$ calc.	78° 33′	135° 54′
$2V_\gamma$ meas.	75°, 80·5°	125–135°
Extinction on (010)	+21½°	+9°
Extinction on (001)	+ 4°	+1°

* The refractive indices and $2V$ are from Emmons (1953) as amended in a private communication from S. W. Bailey (1956); extinctions by R. B. F.

† The refractive indices, $2V$ calc. and $2V$ meas. are from Tuttle & Bowen (1950); extinctions by R. J. T.

Table 3. *Cell dimensions of low and high albites*

	Low albite Ramona, Cal.	High albite (inverted from low form), Amelia, Virginia
$d(100)$ (Å)	7·279±0·005	7·299±0·002
$d(010)$ (Å)	12·752±0·001	12·845±0·001
$d(001)$ (Å)	6·388±0·002	6·353±0·003
α*	86° 20′±02′	86° 06′±02′
β*	63° 32′±02′	63° 38′±02′
γ*	90° 28′±02′	88° 01′±02′
a (Å)	8·138	8·149
b (Å)	12·789	12·880
c (Å)	7·156	7·106
α	94° 20′	93° 22′
β	116° 34′	116° 18′
γ	87° 39′	90° 17′
Volume of cell (Å^3)	664·2	666·7
Cell content	4 [$NaAlSi_3O_8$]	4 [$NaAlSi_3O_8$]
Measured density (g.cm.$^{-3}$)	2·621*	—
Calculated density (g.cm.$^{-3}$)	2·623	2·615
Space group	$C\bar{1}$	$C\bar{1}$

* Emmons, 1953.

as specimen No. 89, 192 in the U. S. National Museum Collection; supplied to Emmons by C. S. Ross. Table 1 gives the chemical composition of this albite and of the Amelia albite used, after inversion, by Traill in his analysis of high albite (Part II). It can be seen that both specimens are nearly pure soda felspar, and in our refinements we have assumed that they are both perfectly pure $NaAlSi_3O_8$. Table 2 gives the optical data for the Ramona low albite and for the Amelia low albite after inversion to the high-temperature form.

The X-ray patterns were obtained from a fragment nearly equidimensional in aspect, with edge ~0·2–0·3 mm., the orientation being fixed by reference to the cleavage planes (010) and (001), identified by observing the extinctions $+21\frac{1}{2}°$ and $+4°$ respectively. Lattice constants determined by the 'θ-method' of Weisz, Cochran & Cole (1948), and in satisfactory agreement with accurate values published earlier for low albites by Cole, Sörum & Taylor (1951), Laves (1952), Baskin (1956), and others, are given in Table 3, together with density, etc. Bailey, Ferguson & Taylor (1951) applied statistical tests to the X-ray intensities of this albite (as well as to an orthoclase and a sanidine) and showed it to be centrosymmetrical; the space group $C\bar{1}$ is appropriate to a cell corresponding exactly with that used originally by Taylor *et al.* (1934). Intensities were obtained from zero-level Weissenberg photographs* taken about each of the three axes using filtered Mo radiation, the standard multiple-film technique and a comparison scale for visual estimation. The intensities are probably accurate to ~±10%. Altogether 125 ($0kl$), 110 ($h0l$) and 121 ($hk0$) reflexions were recorded; for (F_o-F_c) syntheses the inclusion of reflexions of zero intensity with $(\sin\theta/\lambda)^2 \leq 0{\cdot}5$ increased the numbers of terms to 163, 122 and 162 respectively. The measured intensities were corrected graphically for Lorentz and polarization factors (Cochran, 1948); with Mo $K\alpha$ radiation the absorption in the specimen may be neglected. No effects attributable to extinction were observed.

The square roots of the corrected intensities gave a

* In addition, 26 upper-level equi-inclination photographs were taken to provide data for three-dimensional work.

Table 4. *Details of the two-dimensional refinement of low and high albites*

	a axis: $0kl$			b axis: $h0l$		c axis: $hk0$			
Stage of refinement	Type of Fourier	R	Fig.	Type of Fourier	R	Type of Fourier	R	Fig.	Comments
(*a*) Low albite									
0	—	0·33	—	—	0·43	—	0·32	—	Parameters of Taylor *et al.* (1934); f values of Bragg & West (1928)
I	F_o	0·25	—	—	—	F_o	0·21	—	f values unchanged
II	F_o–F_c	0·18	—	—	—	F_o–F_c	0·20	—	f values unchanged
III	F_o–F_c	0·13	2(*a*)	—	0·16	F_o–F_c	0·13	3(*a*)	f values unchanged
IV	F_o–F_c	0·097	—	F_o–F_c	0·11	F_o–F_c	0·096	—	f values unchanged
V	F_o–F_c	0·092	2(*b*)	F_o–F_c	0·080	F_o–F_c	0·093	3(*b*)	f_{Na} changed to B = 1·3 Å^2
VI	F_o–F_c	—	2(*c*)	F_o–F_c	—	F_o–F_c	—	3(*c*)	f_{Na} changed to B = 1·6 Å^2
						F_o	—	1	Final Fouriers: no new parameters derived from them
(*b*) High albite									
0	—	0·35	—	—	—	—	0·37	—	Parameters of Taylor *et al.* (1934); f values of Bragg & West (1928)
I	F_o	0·34	—	F_o	—	F_o	0·28	—	f values unchanged
II	F_o–F_c	0·33	—	—	—	F_o–F_c	0·26	—	f values unchanged
III	F_o–F_c	0·24	—	—	0·17	F_o–F_c	0·15	—	f values unchanged
IV	F_o–F_c	0·19	—	F_o–F_c	0·15	F_o–F_c	0·14	—	f values unchanged
V	F_o–F_c	—	—	F_o–F_c	—	F_o–F_c	—	—	f_{Na} changed to B = 1·5 Å^2
						F_o	—	5	Final parameters derived from Stage V Fouriers

Note: The parameters assumed for any given set of Fouriers except the first were the best derived from the previous set of Fouriers, i.e. at Stage III, for example, refined parameters II were assumed.

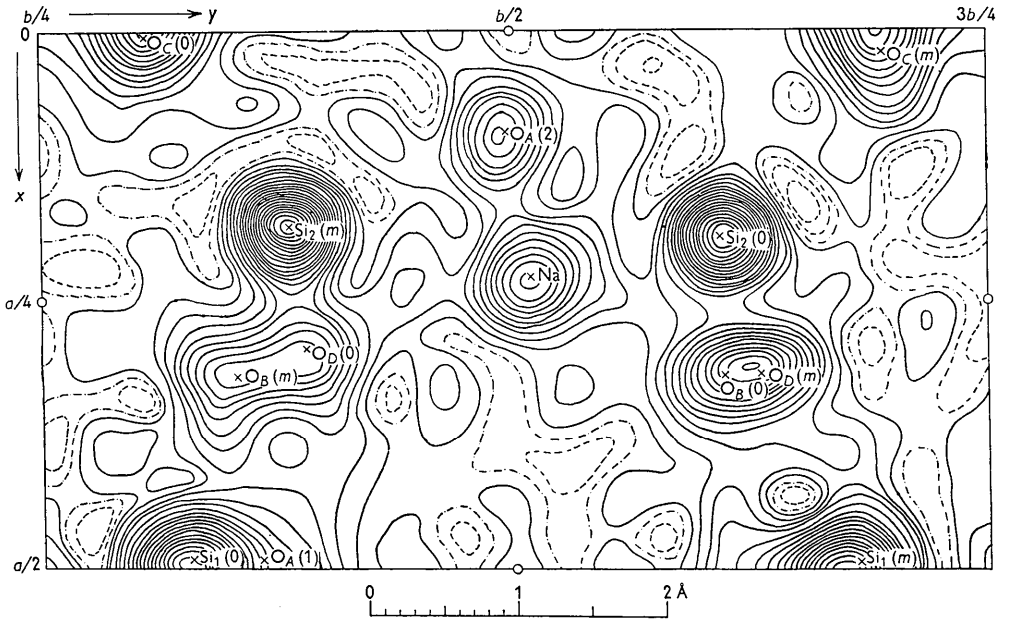

Fig. 1. Low albite, ϱ_o projected along [001], Stage VI. $a' = a \sin\beta = 7{\cdot}279$ Å, $b' = b \sin\alpha = 12{\cdot}753$ Å, $\gamma' = 89° 32'$. Assumed positions denoted by crosses, symmetry centres by open circles. Positive contours in solid line, zero contour in chained line, negative contours in broken line. Contour interval 100 units = 2·155 e.Å^{-2}, except on either side of zero contour (50 units) and in vicinity of atoms $Si_1(0)$, $Si_1(m)$, $O_A(1)$ (200 units).

set of relative F_o's, which were placed on the absolute scale by comparison with structure amplitudes calculated from the parameters of Taylor *et al.* (1934) and the f curves of Bragg & West (1928).* For all four of the tetrahedral (Al, Si) atoms one curve of $(\frac{3}{4}f_{Si}+\frac{1}{4}f_{Al})$ versus $(\sin\theta/\lambda)^2$ was used throughout the refinement. The use of this curve implies a completely random distribution of Al and Si in the tetrahedra, and so avoids any initial assumption that ordering exists. Proceeding in the usual way with the comparison between F_o and F_c for successive small ranges of $(\sin\theta/\lambda)^2$, it gradually became clear as refinement proceeded that the conversion factor was a constant, of the order of 14, for all the reflexions; the value of the factor was checked, and modified if necessary, after each stage in the refinement process.

2. The refinement

The refinement of the structure was carried out by means of F_o and (F_o-F_c) Fourier syntheses of the reflexions in the three principal zones. Most syntheses were of the (F_o-F_c) type, but in the interpretation of these projections certain constants are required from the corresponding F_o projections (Cochran, 1951), and for this reason the first syntheses (along a and c), those based on the parameters of Taylor *et al.* (1934), were of the F_o type. All successive syntheses were of the (F_o-F_c) type until the final stage when an F_o synthesis along the c axis (Fig. 1) was calculated

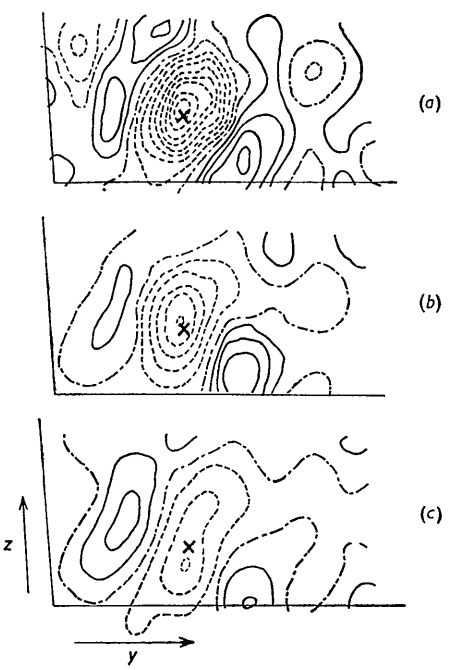

Fig. 2. Low albite, $(\varrho_o-\varrho_c)$ projected along [100], in vicinity of Na atom. $b'=b \sin\gamma=12{\cdot}778$ Å, $c'=c \sin\beta=6{\cdot}400$ Å, $\alpha' = 93° 40'$. Assumed positions denoted by crosses. Convention for positive, zero and negative contours as in Fig. 1. Contour interval 50 units = 1·225 e.Å^{-2}. (*a*) Stage III, (*b*) stage V, (*c*) stage VI.

* The Bragg & West values proved satisfactory, as the refinement proceeded, for all atoms except Na, for which a much larger temperature factor was found necessary. Details relating to this atom are given below.

mainly to provide data for the estimation of the final accuracy. In the (F_o-F_c) syntheses, terms for reflexions with $F_o = 0$ were given half weight in order to allow, in a simple way, for the fact that many reflexions with an observed intensity of zero probably would, with much longer X-ray exposures, be found to have an appreciable intensity. Table 4(*a*) lists the Fourier syntheses that were calculated; other details in the table are referred to below.

Hand calculation with Patterson–Tunell strips in the early stages of refinement was followed by the use of the electronic computer FERUT at the Computation Centre, McLennan Laboratory, University of Toronto, for Fourier syntheses, structure factors, and interatomic distances and bond angles. In Fourier syntheses evaluations were carried out over one quarter of the area of each projection, at intervals $a/60$, $c/60$, and $b/120$ (after Stage III) which give points separated by a little more than 0·1 Å. The contours in Figs. 1, 2 and 3 are in arbitrary units; the conversion factors to absolute units are given in the legends. In locating the maxima on the ϱ_o maps of Stage I the method of Booth (1948) was used, and in calculating the shift of an atom from the $(\varrho_o-\varrho_c)$ maps (Stages II to V) the formula

$$\Delta = \frac{(dD/dr)_{r=0}}{2p\varrho_o(0)} \text{ (Å)}$$

(Cochran, 1951) in which $p = 5{\cdot}0$ Å^{-2} and $\varrho_o(0) =$ 1450, 750 and 950 (arbitrary) units Å^{-2} for Si, O and Na respectively.

The Na atom presented a special problem. In the early $(\varrho_o-\varrho_c)$ projections along a and c (Figs. 2(*a*) and 3(*a*)) this atom was enclosed by a strong negative area bounded on either side, nearly in the y direction, by reasonably strong positive areas. No attempt was made to correct for the anisotropic thermal vibration indicated by the positive peaks, but to correct for the negative trough the value of B in the expression $\exp[-B(\sin\theta/\lambda)^2]$ was increased at Stage V to 1·3 Å^2 from the effective value of Bragg & West (1928) of $\sim 0{\cdot}6$ Å^2. This reduced appreciably the depth of the trough around Na (Figs. 2(*b*) and 3(*b*)), but, because this trough was still marked, B was increased at the final Stage VI to 1·6 Å^2. The effect is shown in Figs. 2(*c*) and 3(*c*). It is unlikely that this situation could be improved by any further changes in B; only an allowance for the anisotropic effect and perhaps a slight shift of the atom could remove the trough and

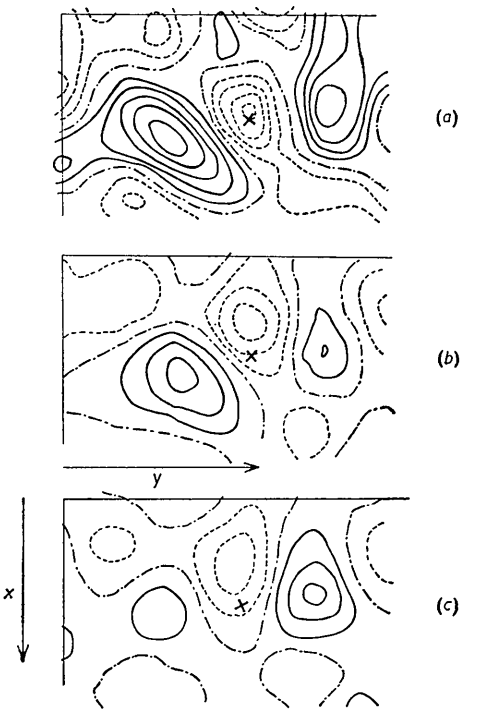

Fig. 3. Low albite, $(\varrho_o-\varrho_c)$ projected along [001], in vicinity of Na atom. Assumed positions denoted by crosses. a', $b'\gamma'$, and convention for positive, zero and negative contours as in Fig. 1. Contour interval 50 units = 1·078 e.Å^{-2}.
(*a*) Stage III, (*b*) stage V, (*c*) stage VI.

Table 5. *Final two-dimensional parameters of low and high albites*

		Low albite			High albite		
		x	y	z	x	y	z
$O_A(1)$	O_{A1}	0·009	0·134	0·967	0·004	0·136	0·981
$O_A(2)$	O_{A2}	0·595	0·997	0·279	0·600	0·990	0·272
$O_B(0)$	O_{B1}	0·818	0·112	0·192	0·808	0·123	0·189
$O_B(m)$	O_{B2}	0·321(0·821)	0·353(0·853)	0·259	0·317(0·817)	0·352(0·852)	0·241
$O_C(0)$	O_{C1}	0·006	0·307	0·268	0·008	0·291	0·266
$O_C(m)$	O_{C2}	0·522(0·022)	0·196(0·696)	0·233	0·520(0·020)	0·188(0·688)	0·220
$O_D(0)$	O_{D1}	0·206	0·110	0·389	0·195	0·112	0·388
$O_D(m)$	O_{D2}	0·683(0·183)	0·369(0·869)	0·430	0·677(0·177)	0·380(0·880)	0·423
$Si_1(0)$	Si_1	0·008	0·171	0·209	0·009	0·165	0·213
$Si_1(m)$	$Si_{1'}$	0·508(0·008)	0·318(0·818)	0·241	0·505(0·005)	0·315(0·815)	0·232
$Si_2(0)$	Si_2	0·692	0·110	0·315	0·690	0·109	0·322
$Si_2(m)$	$Si_{2'}$	0·183(0·683)	0·382(0·882)	0·359	0·184(0·684)	0·377(0·877)	0·354
Na	Na	0·272	0·990	0·145	0·277	0·007	0·140

The atoms are named and numbered, in parallel columns on the left-hand side, first in the standard notation of Megaw (1956) and secondly in the old notation. Where parameters are given in brackets they refer to the type atoms selected by Megaw; the equivalent parameters not in brackets refer to the type atoms of the older convention which in Megaw's notation would be described as $O_B(m0i0)$, $O_C(m0i0)$, etc.

peaks still present. This anisotropic effect shows up on the final $hk0\varrho_o$ map (Fig. 1) but in a much less striking fashion than on the difference maps. The Fourier maps do not yield the exact magnitude of this anisotropic vibration, but they suggest that the maximum separation nearly along y is $\sim 0{\cdot}1$ Å. On the first b-axis projection (Stage IV) a distinct trough surrounded Na but no clear anisotropic vibration was

Table 6. *Interatomic distances and interbond angles of low albite and high albite calculated from the final two-dimensional parameters*

Interatomic distances in Ångström units

			Low albite		High albite		
				Mean values		Mean values	
Si–O	Si_1–O_{A1}		$1{\cdot}76_2$	$1{\cdot}74_2$	$1{\cdot}65_2$	$1{\cdot}65_2$	$1{\cdot}64_5$
	–O_{B1}		$1{\cdot}70_2$		$1{\cdot}65_4$		
	O_{C1}		$1{\cdot}76_2$		$1{\cdot}64_5$		
	O_{D1}		$1{\cdot}74_4$		$1{\cdot}65_8$		
	Si_1'–O_{A1}		$1{\cdot}59_9$	$1{\cdot}59_0$	$1{\cdot}64_6$	$1{\cdot}63_9$	
	O_{B2}		$1{\cdot}62_6$		$1{\cdot}63_3$		
	O_{C2}		$1{\cdot}55_3$		$1{\cdot}64_1$		
	O_{D2}		$1{\cdot}58_3$		$1{\cdot}63_6$		
	Si_2–O_{A2}		$1{\cdot}61_8$	$1{\cdot}63_6$	$1{\cdot}64_6$	$1{\cdot}64_2$	
	O_{B1}		$1{\cdot}62_7$		$1{\cdot}63_5$		
	O_{C2}		$1{\cdot}64_9$		$1{\cdot}64_0$		
	O_{D2}		$1{\cdot}64_9$		$1{\cdot}64_5$		
	Si_2'–O_{A2}		$1{\cdot}64_0$	$1{\cdot}61_6$	$1{\cdot}63_7$	$1{\cdot}64_7$	
	O_{B2}		$1{\cdot}59_7$		$1{\cdot}63_3$		
	O_{C1}		$1{\cdot}61_8$		$1{\cdot}66_8$		
	O_{D1}		$1{\cdot}61_1$		$1{\cdot}64_9$		
Na–O	O_{A1}		$2{\cdot}61_5$		$2{\cdot}64_9$		
			$2{\cdot}68_1$		$2{\cdot}72_1$		
	O_{A2}		$2{\cdot}36_3$		$2{\cdot}38_7$		
			$3{\cdot}66_3$		$3{\cdot}49_2$		
			$3{\cdot}75_9$				
	O_{B1}		$2{\cdot}46_0$		$2{\cdot}61_6$		
	O_{B2}		$(3{\cdot}42_4)$		$(3{\cdot}15_7)$		
	O_{C1}		$2{\cdot}88_9$		$(3{\cdot}30_7)$		
	O_{C2}		$(3{\cdot}24_7)$		$2{\cdot}91_2$		
	O_{D1}		$2{\cdot}46_5$		$2{\cdot}48_1$		
	O_{D2}		$(2{\cdot}99_7)$		$3{\cdot}03_5$		
O–O	Si_1	O_{A1}–O_{B1}	$2{\cdot}72_6$	$2{\cdot}84_2$	$2{\cdot}62_4$	$2{\cdot}69_5$	
		O_{A1}–O_{C1}	$2{\cdot}97_4$		$2{\cdot}74_8$		
		O_{A1}–O_{D1}	$2{\cdot}75_0$		$2{\cdot}64_6$		
		O_{B1}–O_{C1}	$2{\cdot}86_5$		$2{\cdot}58_4$		
		O_{B1}–O_{D1}	$2{\cdot}82_6$		$2{\cdot}83_6$		
		O_{C1}–O_{D1}	$2{\cdot}90_9$		$2{\cdot}73_6$		
	Si_1'	O_{A1}–O_{B2}	$2{\cdot}57_3$	$2{\cdot}59_6$	$2{\cdot}58_9$	$2{\cdot}67_2$	
		O_{A1}–O_{C2}	$2{\cdot}63_2$		$2{\cdot}71_2$		
		O_{A1}–O_{D2}	$2{\cdot}55_5$		$2{\cdot}57_6$		
		O_{B2}–O_{C2}	$2{\cdot}58_6$		$2{\cdot}72_7$		
		O_{B2}–O_{D2}	$2{\cdot}64_1$		$2{\cdot}64_3$		
		O_{C2}–O_{D2}	$2{\cdot}58_9$		$2{\cdot}78_4$		
	Si_2	O_{A2}–O_{B1}	$2{\cdot}68_2$	$2{\cdot}67_0$	$2{\cdot}67_1$	$2{\cdot}67_7$	
		O_{A2}–O_{C2}	$2{\cdot}60_4$		$2{\cdot}64_2$		
		O_{A2}–O_{D2}	$2{\cdot}62_4$		$2{\cdot}61_9$		
		O_{B1}–O_{C2}	$2{\cdot}72_1$		$2{\cdot}59_1$		
		O_{B1}–O_{D2}	$2{\cdot}70_0$		$2{\cdot}70_7$		
		O_{C2}–O_{D2}	$2{\cdot}69_1$		$2{\cdot}83_4$		
	Si_2'	O_{A2}–O_{B2}	$2{\cdot}59_0$	$2{\cdot}63_7$	$2{\cdot}58_1$	$2{\cdot}68_7$	
		O_{A2}–O_{C1}	$2{\cdot}55_6$		$2{\cdot}65_9$		
		O_{A2}–O_{D1}	$2{\cdot}64_6$		$2{\cdot}67_8$		
		O_{B2}–O_{C1}	$2{\cdot}69_2$		$2{\cdot}71_7$		
		O_{B2}–O_{D1}	$2{\cdot}62_9$		$2{\cdot}69_?$		
		O_{C1}–O_{D1}	$2{\cdot}70_7$		$2{\cdot}79_3$		

Table 6 (*cont.*)

Interatomic angles

		Low albite		High albite	
			Mean values		Mean values
O–Si–O	O_{A1}– Si_1 –O_{B1}	103° 48′	109° 22′	105° 03′	109° 28′
	O_{A1}– –O_{C1}	115° 06′		112° 55′	
	O_{A1}– –O_{D1}	103° 20′		106° 09′	
	O_{B1}– –O_{C1}	111° 35′		103° 04′	
	O_{B1}– –O_{D1}	110° 13′		117° 47′	
	O_{C1}– –O_{D1}	112° 09′		111° 51′	
	O_{A1}– $Si_{1'}$ –O_{B2}	105° 48′	109° 17′	104° 16′	109° 10′
	O_{A1}– –O_{C2}	113° 11′		111° 09′	
	O_{A1}– –O_{D2}	106° 48′		103° 24′	
	O_{B2}– –O_{C2}	108° 51′		112° 48′	
	O_{B2}– –O_{D2}	110° 43′		107° 05′	
	O_{C2}– –O_{D2}	110° 18′		116° 18′	
	O_{A2}– Si_2 –O_{B1}	110° 29′	109° 16′	108° 59′	109° 25′
	O_{A2}– –O_{C2}	105° 40′		106° 59′	
	O_{A2}– –O_{D2}	106° 52′		105° 28′	
	O_{B1}– –O_{C2}	112° 17′		104° 34′	
	O_{B1}– –O_{D2}	110° 55′		111° 16′	
	O_{C2}– –O_{D2}	109° 20′		119° 13′	
	O_{A2}– $Si_{2'}$ –O_{B2}	106° 16′	109° 22′	104° 14′	109° 23′
	O_{A2}– –O_{C1}	103° 19′		107° 08′	
	O_{A2}– –O_{D1}	108° 57′		109° 08′	
	O_{B2}– –O_{C1}	113° 42′		110° 46′	
	O_{B2}– –O_{D1}	110° 04′		110° 21′	
	O_{C1}– –O_{D1}	113° 54′		114° 38′	
Si–O–Si	Si_1 –O_{A1}– $Si_{1'}$	141° 54′	139° 25′	144° 24′	139° 39′
	Si_2 –O_{A2}– $Si_{2'}$	130° 47′		133° 07′	
	Si_1 –O_{B1}– Si_2	140° 33′		142° 33′	
	$Si_{1'}$–O_{B2}– $Si_{2'}$	160° 20′		155° 04′	
	Si_1 –O_{C1}– $Si_{2'}$	124° 59′		127° 59′	
	$Si_{1'}$–O_{C2}– Si_2	135° 21′		133° 43′	
	Si_1 –O_{D1}– $Si_{2'}$	133° 53′		136° 03′	
	$Si_{1'}$–O_{D2}– Si_2	147° 35′		144° 18′	

The old notation is used for the atoms; for the corresponding symbols in the new (Megaw) notation, see the left hand side of Table 5.

indicated. The change of B from $\sim 0{\cdot}6$ to $1{\cdot}3$ Å^2 at the next stage brought a zero contour near Na and confirmed the absence of appreciable anisotropic vibration in this projection. In the final b-axis projection where $B = 1{\cdot}6$ Å^2, Na is in a definite positive peak. Apparently in this projection the Na atom has an isotropic thermal vibration with a magnitude corresponding to $B = 1{\cdot}3$ Å^2. This value of B is equivalent to a thermal vibration of amplitude 0·13 Å. The Na atom in low albite may, then, be considered as having an anisotropic thermal vibration which in the plane normal to the y axis is of amplitude 0·13 Å and along y has the greater amplitude suggested by the F_o and (F_o-F_c) Fourier syntheses, namely $0{\cdot}13+\sim 0{\cdot}05 = \sim 0{\cdot}18$ Å. It is worth noting, especially in view of Traill's description in Part II of the nature of the Na atom in high albite, that what is here interpreted as an anisotropic thermal vibration might equally be taken to mean that the Na atom occupies, at random, one or other of two positions within the same cavity which are separated by $\sim 0{\cdot}1$ Å nearly along the y-direction.

Table 4(a) shows, in addition to the Fourier syntheses carried out, the progress of the refinement as indicated by the usual 'reliability' factor $R = \Sigma||F_o|-|F_c|| \div \Sigma|F_o|$. In calculating this factor only those reflexions with $|F_o| > 0$ have been used. As one might expect, the first set of Fourier syntheses (Stage I) yielded parameters which gave much better R factors than those of Taylor *et al.* (1934). The first (F_o-F_c) syntheses (Stage II) produced another marked improvement. The fact that this does not show in Stage II of the $hk0$ projection is due to errors made in the calculation of that synthesis. Stage III of this projection does show a marked improvement. From Stage III onward the rate of improvement was slower. The final values of about 0·09 are close to those reported by Bailey & Taylor (1955) for the comparable stage (the end of the two-dimensional refinement) in their analysis of a triclinic potassium felspar.

The final parameters taken from the Stage V syntheses are given in Table 5. Megaw (1956) has proposed a new system of naming the individual

Table 7. *Final two-dimensional observed and calculated structure factors of low albite and high albite*

The values of $(\sin\theta/\lambda)^2$ for low albite were calculated by desk calculator and checked by the graphical method of Cochran (1948); they are accurate to about ± 2 in the third significant figure. The corresponding values for high albite were determined only by the graphical method and, within the limit of error, are virtually the same as the values for low albite. Thus separate $(\sin\theta/\lambda)^2$ values are not included for high albite.

	low albite		high albite	
h k ℓ	$(\sin\theta/\lambda)^2$	F_o	F_o	F_c
0 0 1	.006	28	-29	0 -16
2	.0245	198	-200	182 -170
3	.055	23	26	29 18
4	.098	45	41	44 31
5	.153	38	34	46 50
6	.221	10	-10	0 -7
7	.300	24	-21	40 -38
8	.392	10	10	0 15
9	.496	16	17	33 35
0 2 0	.006	25	-26	43 -31
4	.025	163	-159	169 -164
6	.055	110	108	109 106
8	.098	61	63	71 77
10	.154	69	77	53 53
12	.221	9	-10	23 -23
14	.301	53	-51	37 -37
16	.394	41	43	28 31
18	.498	33	31	23 24
2 0 0	.019	0	6	0 5
4	.0755	126	122	127 119
6	.170	105	115	122 121
8	.302	0	-4	5 -5
10	.472	57	58	59 63
12	.679	23	22	16 22
14	.925	-	-	0 1
16	1.208	17	21	- -
0 2 1	.013	9	-2	19 -22
2	.032	15	15	14 15
3	.064	36	35	36 32
4	.107	45	-42	45 -48
5	.163	0	0	20 -11
6	.231	35	35	24 30
7	.312	0	-8	7 -5
8	.405	0	-1	0 3
9	.570	34	34	9 26
11	.758	17	-19	- -
12	.898	17	15	- -

	low albite		high albite	
h k ℓ	$(\sin\theta/\lambda)^2$	F_o	F_o	F_c
0 2 $\bar{1}$	.0115	0	0	17 13
2	.029	82	78	82 95
3	.059	17	-20	0 -3
4	.101	87	-90	72 -81
5	.155	64	-61	50 -74
6	.222	26	34	23 25
7	.301	59	62	41 66
8	.392	11	-16	8 -9
9	.495	64	-61	45 -51
10	.611	0	15	- -
11	.740	28	28	- -
12	.880	17	-19	- -
0 4 1	.032	21	25	13 21
2	.052	48	47	35 30
3	.084	41	-45	60 -47
4	.129	24	-24	16 -14
5	.186	61	-55	48 -58
6	.255	0	8	7 -10
7	.336	49	45	35 50
8	.429	0	-2	0 7
9	.535	23	-26	28 -32
0 4 $\bar{1}$	.029	96	95	107 94
2	.046	30	-26	15 -1
3	.075	84	-88	70 -68
4	.116	43	42	43 43
5	.170	0	-6	30 -46
6	.236	36	-37	39 -45
7	.314	12	16	22 26
8	.404	21	25	6 15
9	.508	0	-1	15 -4
0 6 1	.064	69	66	89 85
2	.085	63	-60	68 -74
3	.118	95	-88	110 -111
4	.163	65	64	54 58
5	.220	17	19	46 47
6	.290	59	-61	41 -41
7	.368	0	-1	14 -12
8	.468	22	25	15 16

	low albite		high albite	
h k ℓ	$(\sin\theta/\lambda)^2$	F_o	F_o	F_c
0 6 $\bar{1}$	.056	12	17	6 28
2	.075	102	-97	77 -79
3	.100	0	-12	7 -1
4	.144	61	54	61 50
5	.197	26	26	27 18
6	.259	0	-7	23 -18
7	.333	0	-9	21 -29
8	.422	0	8	6 19
9	.530	31	25	- -
0 8 1	.104	0	10	23 -35
2	.129	27	27	0 -10
3	.163	47	47	72 53
4	.209	49	-49	43 -30
5	.267	16	-14	26 -18
6	.338	22	21	27 26
7	.421	20	17	26 20
0 8 $\bar{1}$	.101	69	-67	61 -25
2	.117	53	49	68 69
3	.144	64	54	69 57
4	.184	76	-90	77 -102
5	.236	27	-23	9 -12
6	.300	59	67	46 48
7	.368	16	15	0 4
8	.465	24	-27	12 -9
11	.808	19	15	- -
0.10.1	.158	0	-4	0 -17
2	.186	43	-46	56 -52
3	.221	53	46	25 26
4	.267	26	-24	10 -15
5	.327	28	-29	20 -19
6	.398	30	32	21 24
7	.480	0	10	0 6
0.10.$\bar{1}$	.156	24	-27	41 -32
2	.170	49	-57	27 -1
3	.191	0	-14	20 18
4	.230	0	10	0 -12
5	.282	0	4	12 -26
6	.351	19	-17	0 -23
7	.417	0	-7	0 7
8	.510	0	13	- -
0.12.1	.232	16	21	9 16
2	.255	17	-14	0 -11
3	.291	43	-44	55 -56
4	.338	19	18	15 8
5	.389	0	11	20 28
6	.465	0	-9	0 -2
7	.555	20	-23	16 -18

	low albite		high albite	
h k ℓ	$(\sin\theta/\lambda)^2$	F_o	F_o	F_c
0.12.9	.760	24	27	- -
0.12.$\bar{1}$	.223	35	35	39 41
2	.236	36	-37	39 -23
3	.262	36	-40	29 -26
4	.301	35	33	46 53
5	.340	0	3	0 -21
6	.414	24	-16	26 -33
7	.489	16	25	8 15
0.14.1	.304	0	-2	22 -14
2	.357	51	56	40 26
3	.373	13	-11	0 -10
4	.410	0	-2	0 11
5	.482	16	-14	0 -1
6	.555	20	-23	22 -22
7	.640	24	25	23 22
8	.735	-	-	17 23
0.14.$\bar{1}$	.302	28	33	40 51
2	.315	27	27	26 23
3	.340	0	-11	7 -4
4	.377	0	-9	0 -6
5	.427	15	-8	8 -12
6	.480	10	18	17 17
7	.563	28	23	26 11
8	.650	-	-	9 -10
0.16.1	.406	16	23	24 12
2	.431	13	-11	12 -20
3	.460	0	0	0 -4
4	.520	-	-	0 3
5	.580	-	-	0 10
6	.652	15	-10	0 3
7	.738	16	12	0 3
8	.835	19	15	- -
0.16.$\bar{1}$	.393	31	-37	45 -35
2	.407	14	-25	0 7
3	.430	20	18	23 30
4	.458	0	6	0 -19
5	.506	0	6	0 6
6	.575	-	-	0 -5
7	.650	24	-25	14 -23
9	.833	22	24	- -
0.18.1	.504	0	12	9 6
2	.537	28	-29	28 -32
3	.575	-	-	0 4
4	.625	-	-	0 -4
6	.761	20	19	- -

	low albite		high albite	
h k ℓ	$(\sin\theta/\lambda)^2$	F_o	F_o	F_c
0.18.$\bar{1}$	.497	30	-32	31 -33
2	.501	0	-10	0 5
3	.540	-	-	9 15
4	.560	-	-	9 -12
0.20.1	.629	20	-20	- -
3	.694	13	23	- -
5	.807	24	-30	- -
0.20.$\bar{1}$	.613	17	22	- -
7	.860	26	21	- -
9	1.04	22	-18	- -
0.22.3	.828	20	-25	- -
0.26.2	1.085	19	-12	- -
3	1.125	19	23	- -
2 0 1	.035	10	11	7 4
2	.0625	33	31	35 38
3	.103	39	-40	56 -49
4	.155	77	76	72 81
5	.220	40	42	54 55
6	.297	42	-47	34 -45
7	.386	23	-25	20 -24
8	.488	15	19	17 15
9	.601	11	10	13 10
10	.725	-	-	0 3
11	.860	-	-	0 -4
2 0 $\bar{1}$	.015	145	145	172 149
2	.024	169	-170	195 -177
3	.045	0	-6	14 -15
4	.079	173	173	196 179
5	.124	21	21	25 33
6	.182	56	-58	44 -39
7	.252	23	-24	12 -21
8	.334	0	4	0 0
9	.429	14	14	18 17
10	.535	-	-	15 11
11	.655	11	-8	13 -14
4 0 1	.101	37	33	35 46
2	.138	139	-136	156 -146
3	.188	18	24	19 14
4	.250	58	66	60 68
5	.325	0	-6	0 -5
6	.411	10	-11	11 -7
7	.510	0	0	0 -6
8	.615	-	-	0 0
9	.744	9	10	17 20
12	1.19	9	-2	- -

	low albite		high albite	
h k ℓ	$(\sin\theta/\lambda)^2$	F_o	F_c	F_o F_c
4 0 $\bar{1}$	.0625	58	48	58 56
2	.062	42	45	63 59
3	.073	130	-122	135 -119
4	.097	6	2	0 3
5	.133	95	89	115 100
6	.181	24	-29	18 -28
7	.241	42	-44	56 -52
8	.314	23	28	19 26
9	.399	19	22	27 33
10	.496	11	-10	- -
11	.606	19	-18	- -
12	1.01	9	-8	- -
6 0 1	.205	52	-50	51 -41
2	.252	8	-14	13 -12
3	.311	16	17	14 12
4	.383	13	14	13 9
5	.467	24	24	32 38
6	.563	13	-15	0 -15
7	.671	20	-25	25 -32
8	.792	9	14	0 14
9	.925	18	15	20 19
10	106	-	-	0 -6
11	1.22	-	-	0 -6
6 0 $\bar{1}$	.147	24	27	30 13
2	.137	127	-129	146 -132
3	.139	19	16	12 20
4	.153	66	62	57 56
5	.179	43	41	44 51
6	.218	0	1	16 19
7	.269	49	-48	44 -44
8	.332	13	-19	16 -18
9	.407	22	22	40 32
10	.495	0	5	14 6
11	.580	-	-	20 -17
12	.707	12	-9	- -
15	1.12	9	-9	- -
8 0 1	.346	21	20	19 17
2	.403	23	-25	23 -25
3	.472	25	-27	25 -33
4	.553	42	44	35 47
5	.647	11	14	0 15
6	.753	25	-26	19 -27
7	.870	-	-	0 0
8	1.00	18	14	0 11
9	1.13	-	-	0 4
10	1.28	-	-	0 0

	low albite		high albite	
h k ℓ	$(\sin\theta/\lambda)^2$	F_o	F_c	F_o F_c
8 0 $\bar{1}$	.270	60	58	59 66
2	.250	6	1	0 -1
3	.242	59	-60	56 -51
4	.247	26	34	39 47
5	.263	22	24	28 22
6	.293	20	-27	21 -31
7	.334	11	-15	10 -11
8	.387	0	3	0 2
9	.453	17	17	12 16
10	.530	-	-	17 20
11	.622	23	-19	- -
17	1.42	11	0	- -
10.0.1	.526	0	-8	0 1
2	.592	48	-47	38 -52
3	.671	31	27	21 24
4	.762	25	24	17 23
5	.865	-	-	0 -7
6	.975	-	-	0 -4
7	1.11	-	-	0 -8
10.0.$\bar{1}$	.430	7	-6	0 -9
2	.400	21	-20	17 -21
3	.383	16	-18	17 -23
4	.378	0	-2	0 -2
5	.385	45	47	46 56
6	.405	0	7	11 10
7	.437	30	-36	32 -37
15	1.13	9	-6	- -
12.0.1	.743	27	-27	21 -26
12.0.$\bar{1}$	.628	39	40	33 37
2	.589	37	-36	33 -37
3	.562	8	-17	0 -8
4	.547	27	27	26 32
5	.555	13	-9	- -
13	.968	15	-11	- -
14.0.4	1.29	12	20	0 18
14.0.$\bar{1}$	.865	13	12	0 15
3	.780	30	-31	24 -35
5	.743	30	30	23 32
7	.755	12	-17	- -

	low albite		high albite	
h k ℓ	$(\sin\theta/\lambda)^2$	F_o	F_c	F_o F_c
16.0.1	1.29	12	-15	- -
16.0.$\bar{5}$	.980	13	11	- -
7	.973	13	-16	- -
1 1 0	.006	20	17	19 10
3	.018	81	-86	97 -102
5	.042	9	0	12 -25
7	.080	35	30	13 3
9	.129	72	-72	94 -104
11	.190	24	27	19 9
13	.264	27	25	25 15
15	.350	30	-20	22 -33
17	.450	0	11	11 -14
$\bar{1}$ 1 0	.006	26	16	34 29
3	.019	104	-109	121 -101
5	.043	43	-38	34 -22
7	.080	43	34	67 78
9	.130	67	-62	41 -28
11	.194	0	-9	5 10
13	.269	0	-7	0 6
15	.351	27	-24	10 0
17	.452	0	17	16 28
2 2 0	.025	127	-122	133 -118
4	.043	58	62	82 69
6	.074	77	75	89 75
8	.117	130	-133	111 -108
10	.171	0	-4	14 9
12	.239	42	39	36 45
14	.319	17	-25	0 -13
16	.421	18	8	11 5
18	.519	0	-4	0 11
$\bar{2}$ 2 0	.025	129	-126	133 -128
4	.044	46	47	52 44
6	.075	107	101	95 78
8	.118	120	-128	126 -134
10	.173	33	-31	41 -49
12	.241	42	41	47 44
14	.321	0	5	14 13
16	.412	0	6	11 -20
18	.519	29	-30	30 -30

Table 7 (*cont.*)

h k ℓ	(sinθ/λ)²	low albite F_o	low albite F_c	high albite F_o	high albite F_c
3 1 0	.044	43	48	52	54
3	.057	35	-36	33	-26
5	.081	10	-4	0	9
7	.117	33	29	47	56
9	.166	20	-15	8	-5
11	.227	20	29	20	32
13	.301	29	-34	27	-17
15	.386	35	-32	21	-16
17	.484	45	47	32	39
$\bar{3}$ 1 0	.044	48	42	52	45
3	.057	0	-11	22	-19
5	.082	0	11	20	6
7	.119	43	35	30	28
9	.168	13	10	8	-18
11	.230	35	42	27	26
13	.304	15	-11	14	-13
15	.390	26	-11	0	-20
17	.489	43	44	24	18
4 2 0	.0813	57	-60	67	-66
4	.0994	14	-6	7	-10
6	.130	81	79	70	70
8	.172	40	-45	54	-56
10	.228	0	10	0	-10
12	.295	24	29	25	25
14	.370	0	-10	0	-1
16	.470	0	14	-	-
$\bar{4}$ 2 0	.082	39	-41	47	-45
4	.101	30	-26	28	-28
6	.132	51	52	49	57
8	.175	37	-43	23	-18
10	.231	24	30	18	23
12	.300	0	8	7	7
14	.379	45	-47	34	-33
16	.472	21	17	-	-
5 1 0	.119	24	20	13	18
3	.131	46	-50	55	-57
5	.155	37	39	32	20
7	.192	38	39	33	30
9	.241	48	-55	54	-61
11	.302	24	23	17	11
13	.375	30	22	18	11
15	.462	0	-8	-	-
$\bar{5}$ 1 0	.120	17	10	15	16
3	.132	39	-37	42	-40
5	.157	32	32	48	38
7	.195	23	13	22	30
9	.244	57	-59	52	-53
11	.305	0	9	21	19
13	.380	33	25	29	34
15	.467	0	-9	-	-
6 2 0	.175	75	-73	68	-67
4	.193	86	-93	92	-83
6	.224	20	26	28	32
8	.267	0	-9	0	7
10	.319	0	10	20	21
12	.388	27	-22	22	-18
14	.468	48	-52	38	-36
$\bar{6}$ 2 0	.177	39	-41	44	-42
4	.196	87	-85	88	-94
6	.227	24	23	17	19
8	.270	0	-13	0	-5
10	.324	0	13	0	-7
12	.390	0	-2	0	-9
14	.475	29	-28	11	-17
7 1 0	.232	38	40	39	36
3	.244	23	-29	19	-24
5	.268	30	28	29	33
7	.304	20	19	17	23
9	.353	24	-27	24	-28
11	.414	29	33	30	37
13	.490	0	1	0	13
7 1 0	.233	42	37	48	42
3	.246	24	-25	29	-32
5	.272	0	12	0	1
7	.309	33	28	22	27
9	.355	0	7	0	1
11	.418	0	17	0	6
13	.498	0	-9	23	-21
8 2 0	.307	12	-19	26	-28
4	.325	54	51	45	45
6	.355	42	44	35	36
8	.398	63	-67	66	-72
10	.450	0	-2	0	-9
12	.519	40	47	28	34
$\bar{8}$ 2 0	.309	33	-35	26	-27
4	.328	32	32	37	39
6	.359	51	56	49	56
8	.403	45	-50	35	-41
10	.459	23	-20	16	-15
12	.528	23	23	25	37
9 1 0	.377	0	10	0	10
3	.395	45	-46	39	-47
5	.414	0	1	0	-3
7	.455	0	10	-	-
9	.504	0	-15	-	-
$\bar{9}$ 1 0	.382	0	11	0	12
3	.397	32	-30	33	-37
5	.422	0	-4	0	-1
7	.461	0	-7	-	-
9	.512	0	-14	-	-
10 2 0	.477	30	-25	16	-22
4	.498	33	-31	23	-23
6	.525	26	25	27	30
$\bar{10}$ 2 0	.482	0	0	0	-3
4	.498	30	-29	32	-38
6	.520	-	-	0	8
$\bar{11}$ 1 0	.575	0	-4	-	-
3	.586	13	-12	-	-
5	.612	21	26	-	-
7	.650	20	6	-	-
9	.700	27	-23	-	-

atomic sites in the felspar structures in an attempt to standardize the descriptions of these structures. For albite she has proposed that no change be made in existing usage in defining the sites of atoms O_{A1}, O_{A2}, O_{B1}, O_{C1}, O_{D1}, Si_1, Si_2 and Na; the prototypes of these atoms remain (0000) in her notation. For the remaining atoms, O_{B2}, O_{C2}, O_{D2}, $Si_{1'}$ and $Si_{2'}$ she has suggested that the prototypes be (m000) and not ($m0i0$) as in the past. The co-ordinates of the former are related to those of the latter by an addition of $\pm 0{\cdot}5$ to x and y, with z remaining unchanged. Because all our work has been done with the older prototype ($m0i0$) of these atoms we give our parameters with reference to it in Table 5 without parentheses, but in parentheses we give the parameters of the atoms with reference to (m000) as prototype. Finally, in Table 6 are given the interatomic distances and interbond angles calculated from the parameters given in Table 5, and in Table 7 are given the final F_o and F_c values.

3. Accuracy and conclusions

The R factors given in Table 4(a) indicate in a general way the accuracy of the results, the final values of $\sim 9\%$ suggesting that the refinement has been carried about as far as is justified by the accuracy of the intensity measurements.

The distribution of Al and Si atoms in the tetrahedra may be deduced from the interatomic distances listed in Table 6 by means of Smith's (1954) curve of (Al, Si) content against size of tetrahedron, as follows:

Tetrahedron	Mean bond length (Å)	Al content
$Si_1(0)$	1·742	0·80
$Si_1(m)$	1·590	0
$Si_2(0)$	1·636	0·22
$Si_2(m)$	1·616	0·10
	Total	1·12

Table 8. *Analysis of the accuracy of results of the two-dimensional syntheses of low and high albites*

	Low albite		High albite	
$-C_n$ (e.Å^{-4}) O	303		280	
$-C_n$ (e.Å^{-4}) Si	845		629	
$-C_n$ (e.Å^{-4}) Na	365		—	
$\sigma(y)$ (Å) O	0·018		0·016	
$\sigma(y)$ (Å) Si	0·006		0·007	
$\sigma(y)$ (Å) Na	0·015		—	
σ(Si–O) (Å)	0·019		0·018	
$\delta l/\sigma$ $Si_1(0)$–$Si_1(m)$	5·76	Significant	0·52	Not significant
–$Si_2(0)$	4·02	Significant	0·40	Not significant
–$Si_2(m)$	4·77	Significant	0·20	Not significant
$Si_2(0)$–$Si_1(m)$	1·74	Possibly significant	0·12	Not significant
–$Si_2(m)$	0·76	Not significant	0·20	Not significant
$Si_1(m)$–$Si_2(m)$	0·99	Not significant	0·32	Not significant
For Al–O = 1·78±0·02 Å and Si–O = 1·60±0·01 Å (Smith, 1954)			For $(Si_{\frac{3}{4}}Al_{\frac{1}{4}})$–O = 1·642±0·008 Å (Cole *et al.*, 1949)	
	σ (Å)	$\delta l/\sigma$		
$Si_1(0)$–[Al–O]	0·027	1·39	Not significant	1·645±0·018–[$(Si_{\frac{3}{4}}Al_{\frac{1}{4}})$–O]
$Si_1(m)$–[Si–O]	0·021	0·47	Not significant	σ = 0·020 Å $\delta l/\sigma$ = 0·15
$Si_2(0)$–[Si–O]	0·021	1·70	Possibly significant	Not significant
$Si_2(m)$–[Si–O]	0·021	0·76	Not significant	

The fact that the total Al content is appreciably greater than unity is presumably due to the possible error in both the mean bond lengths and the graph.

The significance to be attached to these comparisons of bond lengths is brought out more clearly by the application of the statistical tests of Cruickshank (1949) in the manner recommended by Lipson & Cochran (1953). The standard deviation of errors in the atomic parameters was derived from the final (Stage VI) ϱ_o and $(\varrho_o-\varrho_c)$ c-axis projections, using the expression $\sigma(y_n) = \{\overline{(dD/dy)^2}\}^{\frac{1}{2}}/C_n$, where $D = \varrho_o-\varrho_c$ and C_n is the central curvature at the centre of the nth atom. By evaluating $\sigma(y)$ over the whole cell (the first of the two procedures suggested by Lipson & Cochran (1953, p. 308)), errors due to 'residual gradients', which might be removed by further small changes in parameters, and those due to a wrongly-assumed electron distribution around the Na atom, have been included in the experimental errors. No allowance has been made for computational errors, which the analyses of sanidine and microcline showed were negligible in relation to the experimental errors, even for a three-dimensional refinement. Table 8 lists the values of $\sigma(y)$ for Si, O and Na atoms. The standard deviation of error is assumed to be the same in all directions, and no account is taken of the asymmetry of the Na atom. The value of σ(Si–O) for the Si–O tetrahedral distances is also shown in Table 8.

Cruickshank's significance levels are expressed in terms of the probability P that by chance a bond length A could be observed as greater than a bond length B by at least δl, although really equal to B. With $\sigma^2 = \sigma^2(A)+\sigma^2(B)$,

if $P \geq 5\%$, $\delta l/\sigma \leq 1{\cdot}645$, difference not significant,
if $5\% > P > 1\%$, $2{\cdot}327 > \delta l/\sigma > 1{\cdot}645$, difference possibly significant,
if $1\% > P > 0{\cdot}1\%$, $3{\cdot}090 > \delta l/\sigma > 2{\cdot}327$, difference significant,
if $P < 0{\cdot}1\%$, $\delta l/\sigma > 3{\cdot}090$, difference highly significant.

In Table 8 the values of $\delta l/\sigma$ are set out first for the comparison of the (Al, Si)–O distances with each other, second for comparison of these distances with Smith's values for Al–O (tetrahedron $Si_1(0)$) and Si–O (tetrahedra $Si_1(m)$, $Si_2(0)$ and $Si_2(m)$). Smith's stated 'accuracy' of $\pm 0{\cdot}02$ Å for the Al–O distance, and $\pm 0{\cdot}01$ Å for Si–O, is assumed to be the standard deviation of his error.

The figures in Table 8 show clearly that, within the limits of accuracy of the analysis, site $Si_1(0)$ is occupied largely by Al atoms, sites $Si_1(m)$ and $Si_2(m)$ largely or entirely by Si atoms, while site $Si_2(0)$ may have a small amount of Al replacing the dominant Si. In this case, the Si displaced from $Si_2(0)$ has presumably been transferred to $Si_1(0)$. The three-dimensional refinement is expected to show beyond doubt whether or not a small amount of Al is present in site $Si_2(0)$.

It is of interest to note at what stage of the refinement the true nature of the Al–Si ordering became apparent. This is shown by the following tabulation:

Stage of refinement	*R* factors			Average sizes of tetrahedral 'holes' (Å)			
	a	*b*	*c*	$Si_1(0)$	$Si_1(m)$	$Si_2(0)$	$Si_2(m)$
II	0·18	—	0·20	1·68	1·60	1·70	1·61
III	0·13	0·16	0·13	1·76	1·61	1·65	1·59
IV	0·097	0·11	0·096	1·74	1·58	1·64	1·61
V	0·092	0·080	0·093	1·74	1·59	1·64	1·62

Thus in this case of a high degree of Al–Si ordering, the nature of the ordering was apparent as early as Stage III although further refinement was necessary to verify this.

In summary, three principal conclusions may be drawn from this two-dimensional refinement of the structure of low albite:

1. The Si and Al atoms are highly ordered with Al occupying site $Si_1(0)$. A small amount of Al may be present in site $Si_2(0)$, a corresponding amount of Si being present in site $Si_1(0)$.
2. The Na atom has a real or apparent anisotropic thermal vibration: in a direction roughly parallel to the y axis its amplitude is perhaps 0·05 Å greater than in the plane normal to the y axis. This anisotropic thermal vibration may also be interpreted as meaning that the Na atom occupies, at random, one or other of two positions within the same cavity which are separated by $\sim 0{\cdot}1$ Å roughly along y.
3. The Na atom has, furthermore, a much higher degree of thermal vibration even normal to the y axis than that implied in the scattering factor of Bragg & West (1928), the former corresponding to $B = 1{\cdot}3$ Å^2, the latter to $B \sim 0{\cdot}6$ Å^2.

The writer of this part of the paper acknowledges the generous help of Dr Taylor, who suggested the problem, provided the material, and directed the general course of the investigation. Many helpful discussions were held with Dr Traill, and valuable assistance was provided at various times during the course of the research by Drs J. V. Smith, S. W. Bailey and W. Cochran. He is indebted to Drs C. C. Gotlieb and J. Kates of the Computation Centre, University of Toronto, for carrying out many of the computations, and to Dr V. Schomaker and Dr O. F. Tuttle for advice on methods of computation and for help in connexion with the acquisition of felspar material. Much compilation and desk calculation were patiently done in Cambridge by Mrs Margaret Ferguson and Mrs Helen Rodney, and in Winnipeg by Mrs Ferguson and Miss Norma Tweedy. He is grateful to the National Research Council (of Canada) for a Postdoctoral Overseas Fellowship and for several generous research grants.

PART II. HIGH ALBITE*

By R. J. TRAILL

1. Experimental details

The crystal used for the structure analysis was a low-temperature albite from Amelia County, Virginia, which was inverted to the high-temperature form by heating. The natural specimen was obtained from R. C. Emmons of the University of Wisconsin, who in turn had obtained it from C. S. Ross of the U. S. Geological Survey. This albite is specimen No. 31 in the suite of felspars described chemically, optically and petrologically by Emmons (1953). The chemical analysis, as reported by C. S. Ross in Emmons (1953), is given in Table 1, and shows the mineral to be nearly pure $NaAlSi_3O_8$.

A few fragments of the specimen were heated at a temperature of 1065° C. for 16 days. The heated albite was examined optically, after cooling, by the writer to determine whether the inversion had taken place. Extinction angles measured on the (010) and (001) faces were found to be about 9° and 1° respectively, in agreement with the values for high albite recorded by Tuttle & Bowen (1950). Confirmation that the inversion had taken place was obtained by comparing X-ray powder diffraction data for the heated and unheated specimens. The measured spacings and estimated intensities for the heated material are in close agreement with the data for high albite listed by Tuttle & Bowen (1950). The line at $d = 3{\cdot}01$ Å which Tuttle & Bowen consider to be diagnostic of the high-temperature form is present in the pattern of the heated albite and does not occur in the pattern of the unheated material. There was no doubt that the inversion from low- to high-temperature albite had taken place.

Most of the high albite proved to be twinned polysynthetically, but it was possible to isolate a few fragments optically free from twinning; one of these, about 0·1 mm. on each edge, was found to give single-crystal X-ray patterns and was finally selected for the structure analysis. The orientation of the crystal was fixed in the first instance by reference to the cleavage planes (010) and (001), identified from their extinction angles +9° and +1° respectively; precise alignment in the X-ray camera was achieved by the methods of Weisz & Cole (1948).

The dimensions of the unit cell, chosen to correspond with the cell of low albite, were determined by the θ-method of Weisz *et al.* (1948) using the reflexions 600, 0,16,0, and 007. The mean values from a number of independent determinations are collected in Table 3, together with the calculated density etc.

Intensities were estimated visually, with a comparison scale, on Weissenberg equi-inclination photographs taken with filtered Mo radiation, using the standard multiple-film technique. Altogether about 15,000 intensities were measured, for 2200 different reflexions (hkl) appearing on 22 layer lines around the a, b and c axes; of these only the reflexions on the three zero-layer patterns ($0kl$), ($h0l$) and ($hk0$) were used in the present two-dimensional analysis.

The statistical test of Howells, Phillips & Rogers (1950) applied to the measured intensities of 512 reflexions with indices ($hk1$) and ($1kl$) shows that high albite is centrosymmetrical (Fig. 4). Space group $C\bar{1}$ is chosen, rather than $P\bar{1}$, to conform with low albite.

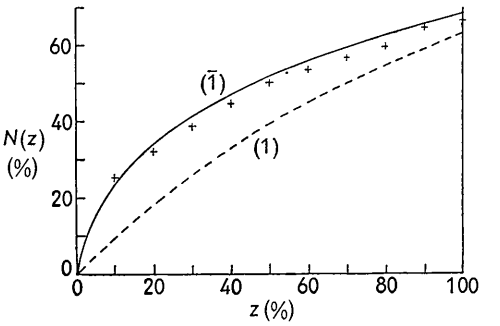

Fig. 4. $N(z)$ test for centrosymmetry in high albite. Experimental points are indicated by crosses. The theoretical curve for centrosymmetry is indicated as a solid line, that for non-centrosymmetry as a dashed line.

The measured intensities were corrected for Lorentz and polarization factors and were converted to absolute F_o values, as described by Ferguson in Part I. The atomic parameters of Taylor *et al.* (1934) and the f values of Bragg & West (1928) were used to calculate the first set of structure factors. Improved parameters were used as the refinement proceeded, and an increased temperature factor was applied to the f values for the Na atom in the later stages of the refinement.

2. The refinement

The structure of high albite was refined by successive two-dimensional F_o and (F_o-F_c) Fourier syntheses, which are listed in Table 4(b). The reasons for using both F_o and (F_o-F_c) syntheses are given by Ferguson in Part I and need not be repeated here.

Details of the procedure during refinement are available in the author's Ph.D. Thesis: in general the account given in Part I for low albite is also applicable to high albite, e.g. in regard to the numbers of terms ($0kl$), ($h0l$) and ($hk0$), to the areas of projection and the intervals chosen for computation, and to the methods used in deriving information about atomic shifts at each stage of the refinement. The R values quoted in Table 4(b) serve to indicate the progress made at each stage.

In all the $(\varrho_o-\varrho_c)$ maps prepared to Stage IV, the Na atom is located in a deep electron-density depression flanked on one or both sides, more or less along y,

* Extracted from an unpublished Ph.D. Thesis: *The Atomic Structure of High-Temperature Albite.* Queen's University. 1956.

by marked positive areas. In an attempt to reduce this persistent trough, a larger empirical temperature factor was introduced into the scattering factor of the Na atom at Stage V. The revised f values were obtained by multiplying the Hartree values by a Debye–Waller temperature factor, $\exp[-B(\sin\theta/\lambda)^2]$, with $B = 1{\cdot}5$ Å^2. This value of B is approximately twice that which is incorporated in the experimentally derived Bragg & West f values for Na. Final (F_o-F_c) syntheses were then computed over the same projected areas and summation intervals as the Stage IV syntheses, and in addition an F_o synthesis was made along the c axis (Fig. 5), mainly to provide data for estimating the accuracy of the analysis. These maps showed that increasing the temperature factor of Na to $B = 1{\cdot}5$ Å^2 changed only slightly the magnitude of the depressions occupied by that atom in the $(\varrho_o-\varrho_c)$ projections along the a and c axes, but resulted in a large decrease in the magnitude of the depression in the b-axis projection. The persistence of the latter depression, however, indicates that the thermal vibration of the Na atom is greater than in low albite. From a consideration of the troughs and associated peaks in the vicinity of the Na positions it is apparent that the final x and z parameters are substantially correct but that no single choice of the y parameter could eliminate the anomalies around Na in the $(\varrho_o-\varrho_c)$ maps or the pronounced elongation of the electron-density curves around it on the ϱ_o map. These characteristics of the Fourier maps indicate that the Na atom either has an exceedingly strong anisotropic thermal vibration nearly along y, or that it occupies, at random throughout the structure, one side (nearly along y) of one-half of the available cavities and the other side of the remaining cavities. The latter seems the more reasonable interpretation, and, because of its interest, is discussed in greater detail below. However, a set of parameters describing the best average position of Na has been deduced by taking, as the maps suggest, values intermediate between those used for the Stage IV and Stage V Fourier syntheses, and these values are given in Table 5 along with final parameters for all the other atoms taken from the final Stage V maps. Where two sets of parameters are given in the table, those without parentheses refer to the prototype ($m0i0$) and those in parentheses refer to prototype ($m000$), according to the notation proposed by Megaw (1956) to standardize the naming of atomic sites in felspar structures. A list of the interatomic distances and interbond angles calculated from the final parameters is given in Table 6, and the F_o and F_c values used for the Stage V refinement are compared in Table 7. F_c values were not computed from the final parameters and thus a comparison of the final values cannot be given.

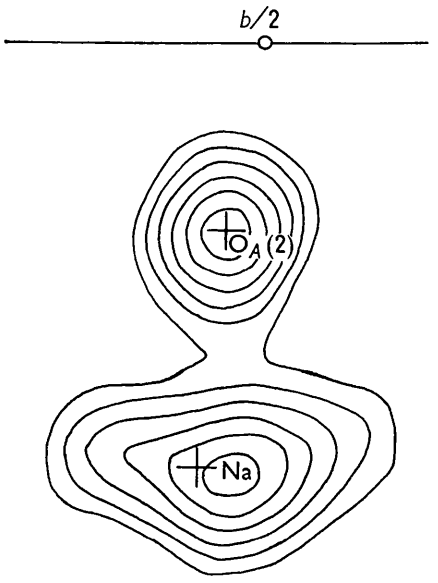

Fig. 5. High albite, ϱ_o projected along [001], Stage V. Contour interval 100 units = 2·13 e.Å^{-2} around the Na atom. Negative contours omitted. Compare with the corresponding portion of Fig. 1 for low albite and note especially the elongation (along y) of the contours of the sodium atom.

3. Accuracy and conclusions

The standard deviations of errors in the atomic parameters and in the tetrahedral interatomic distances have been determined by the same methods as with low albite, and Cruickshank's significance tests have also been applied; the results are shown in Table 8. No analysis of error in the sodium parameters was attempted because of the marked asymmetry of that atom.

The application of Cruickshank's significance levels (Table 8) shows that the differences between the four mean tetrahedral distances are not significant, and that the mean value of the 16 measured bond lengths (1·645 Å) is not significantly different from the mean value, 1·642 Å, of the 16 tetrahedral bond lengths measured in sanidine by Cole *et al.* (1949). The mean value in high albite is, like that in sanidine, consistent with a statistical distribution of $(\frac{3}{4}\,\mathrm{Si}+\frac{1}{4}\,\mathrm{Al})$ in each tetrahedral site, and it is thus concluded that the structure of high albite is characterized by a random distribution of Al and Si atoms throughout the 16 tetrahedral sites.

It was noted earlier that the final Fourier maps indicate that the cavity available for Na is much larger than this atom can fill and that it probably occupies one side (along y) of one-half the available cavities and the other side of the remaining cavities. This being so, a more realistic set of Na–O distances than that given in Table 6 is probably obtained by assuming one set of parameters for one-half the sodiums and another set for the other half, the two sets of parameters describing the extreme positions in the cavity which Na is able to occupy. The exact amount of this separation cannot be deduced from the Fourier maps, but they suggest and the resultant Na–O distances

confirm that a separation of 0·6 Å along y is reasonable. The sum of the ionic radii Na^+ and O^{2-} is 2·35 Å, and if it is assumed that the Na atom can move 0·3 Å to either side along y of the position listed in Table 5, it is found that no Na–O distances are less than 2·35 Å. The two extreme Na positions have therefore been chosen 0·6 Å apart along y, and the Na–O distances calculated for these two positions are given in Table 9. The Na–O distances in Tables 6 and 9 are referred to again in Part III, where charge distributions are discussed, but it may be noted here that in both low and high albite Na can be regarded as having about six or seven closest neighbours. If only the six contacts of ~ 2·9 Å or less are included, then a comparison of Table 9 with Table 6 shows, as one would expect, that the oxygens enclose the extreme Na positions more closely than they do the average Na position.

Table 9. *Interatomic distances between the oxygen atoms and the two extreme positions of sodium in high albite*

(Distances in Ångström units)

Atoms	Na′	Na″
Na–$O_A(1)$	2·46 (3)	2·85 (5)
Na–$O_A(1')$	2·92 (6)	2·53 (3)
Na–$O_A(2)$	2·44 (2)	2·37 (1)
Na–$O_A(2')$	3·49	3·52
Na–$O_B(0)$	2·80 (5)	2·45 (2)
Na–$O_B(m)$	2·98 (7)	3·35
Na–$O_C(0)$	3·57	3·05 (7)
Na–$O_C(m)$	2·68 (4)	3·15
Na–$O_D(0)$	2·35 (1)	2·64 (4)
Na–$O_D(m)$	3·22	2·87 (6)

Notes: (*a*) In the above table the two sodium positions are separated by 0·6 Å in the y direction. The parameters are:

Na′: $x = 0{\cdot}277$, $y = 0{\cdot}030$, $z = 0{\cdot}140$;
Na″: $x = 0{\cdot}277$, $y = -0{\cdot}016$, $z = 0{\cdot}140$.

(*b*) The numbers in parentheses show the orders of increasing Na–O distance of the seven closest oxygens in each case.

(*c*) Two oxygen atoms of type $A(1)$ make contacts with the sodium atom, and are distinguished as $O_A(1)$ and $O_A(1')$; similarly for atoms $O_A(2)$ and $O_A(2')$; compare figures in Table 6.

In summary, the following conclusions may be drawn from this two-dimensional analysis of the structure of high albite:

1. The Al and Si atoms are randomly distributed among the four tetrahedral sites, resulting in a completely disordered arrangement.

2. The Na atom does not occupy a single fixed position throughout the structure but instead it occupies, at random, one side along y of one-half the available cavities and the other side of the remaining cavities, the separation of the two extreme positions being ~ 0·6 Å. The large size of the cavity presumably results, directly or indirectly, from the random distribution of the Al–Si atoms.

3. The Na atom has a much higher degree of thermal vibration than that implied in the scattering factor of Bragg & West (1928), and also an appreciably greater thermal vibration than the Na atom in low albite.

The author is indebted to Dr Ferguson for suggesting the problem and generally directing the research, and to Dr L. G. Berry of the Department of Geological Sciences, Queen's University, Kingston, Ontario, for further guidance and for help with some of the Fourier calculations. He is grateful to Mr S. A. Forman, formerly of the Department of Mines and Technical Surveys, Ottawa, Ontario, for heat-treating the specimen used in this investigation, and to Drs C. C. Gotlieb and J. Kates of the Computation Centre, University of Toronto, for doing many of the computations. He acknowledges with thanks generous financial support from the National Research Council (of Canada) in the form of studentships and research grants.

PART III. DISCUSSION

1. Comparison of sodium felspar and potassium felspar structures

Tables 5 and 6 show that the structures of low and high albites are closely similar, as was strongly suggested by the similarity in optical properties and cell dimensions.

The interatomic distances and interbond angles for the albites (Table 6) may be compared with those for microcline (Bailey & Taylor, 1955, their Table 8), and for sanidine (Cole *et al.*, 1949, their Table 4). In comparing the triclinic structures with the monoclinic sanidine, it must be kept in mind that pairs of sites $Si_1(0)$ and $Si_1(m)$, $Si_2(0)$ and $Si_2(m)$, $O_B(0)$ and $O_B(m)$, etc. which are non-equivalent in the triclinic structures constitute single sites Si_1, Si_2, O_B etc. in the monoclinic structure. Comparison of the microcline structure with that of low albite involves a complication arising from the arbitrary choice of positive directions for the axes of a triclinic crystal. The difficulty of selecting axes which are structurally comparable for microcline and low albite is enhanced because both cells depart only slightly from monoclinic symmetry. Laves (1951) has given reasons for supposing that structural equivalence with the conventional albite cell is *not* achieved when the conventional microcline axes are used, but that the microcline axes must be rotated 180° around b. Accepting this viewpoint, for comparison with albite it becomes necessary to interchange the pairs of sites $Si_1(0)$ and $Si_1(m)$, $Si_2(0)$ and $Si_2(m)$, $O_B(0)$ and $O_B(m)$, etc. of the microcline structure as described by Bailey & Taylor (1955), who accepted the conventional axial orientation; for example the tetrahedral group $Si_1(0)$ of albite (Si_1 in the old notation) as described in the present paper should be compared with the tetrahedral group $Si_1(m)$ ($Si_{1'}$ in the old notation) of microcline as described by Bailey & Taylor. It must be emphasized

that this choice of the basis of comparison of two structures, both near monoclinic, is dependent not on any *convention* concerning axial angles but on the experimental observations reported by Laves.

Comparison of these four structures shows that there are very striking similarities between the two pairs of felspars:

(*a*) The high-temperature minerals, sanidine and high albite, are characterized by complete disordering of the Al–Si atoms, whereas the low-temperature minerals, microcline and low albite, are characterized by a fairly high degree of Al–Si order. The degree of ordering is higher in low albite than in the particular microcline examined by Bailey & Taylor, but the close similarity between the two structures nevertheless persists in that, in both minerals, the highest concentration of Al is found in structurally equivalent sites, $Si_1(m)$ in microcline and $Si_1(0)$ in low albite. Towards the end of the paper we show that it is possible to suggest a reason for the close similarity between the low albite and microcline structures.

(*b*) The alkali atoms in both low-temperature forms have about the same degree of thermal vibration, the B value for K in microcline being 1·0 Å^2 and for Na in low albite 1·3 Å^2. Furthermore, in both high-temperature forms the alkali atoms have a much higher degree of thermal vibration than in their corresponding low-temperature forms, the K in sanidine having a B value of 1·9 Å^2 (Bailey & Taylor, 1955) and the Na in high albite a value which, although not determined, is probably near this.

An important difference between the K and the Na felspar structures is that in the former the K atom shows no signs of anisotropic thermal vibration whereas in the albites the Na atom shows effects equivalent to anisotropic vibration (nearly along y), to a small degree in low albite but to a very high degree in high albite. This difference in the behavior of the two alkali atoms is presumably due to the fact that the large K atom can fill the large cavity whereas the small Na atom cannot fill it completely. The physical interpretation of the effective anisotropic vibration of the Na atom requires discussion. In the first place, the effect may in fact be a thermal vibration, with a moderate degree of anisotropy in low albite and a high degree of anisotropy in high albite. Alternatively, as has already been suggested in Parts I and II, the Na atom may occupy at random through the structure one or other of two positions, within the same large cavity, separated by ~0·1 Å (in low albite) or ~0·6 Å (in high albite), in a direction nearly along y. In this case the randomness may represent either a space average—each Na atom remaining in its own position within the cavity—or a time average—each Na atom spending part of its time in one position, part in the other, within the cavity. It may be possible to say more about this when the three-dimensional syntheses are completed. Experiments at low temperature would also be instructive.

2. Electrostatic charge distributions in low and high albites

The stability of an ionic structure may be discussed in terms of 'electrostatic valence' or local balance of charges; on this view the strengths of the positive bonds contributed to each oxygen ion O^{-2} should total 2, and the more nearly this requirement is satisfied the more stable is the structure. Similarly, bond strengths contributed to the four oxygens constituting a tetrahedral SiO_4 or AlO_4 group should total 8. Arguments based on this idea of charge balance must be accepted with some caution in the case of the felspars. In the first place the structures are very complex, so that the chance of achieving the ideal balance is reduced by comparison with simpler and more regular coordination groupings. Secondly, it seems likely that some of the bonds in silicates, and in particular those within the tetrahedral SiO_4 group, may be at least partly covalent in character. Thirdly, especially in the high-temperature materials, we can discuss only *averages* for a random Al–Si distribution within a given tetrahedron, whereas in fact there must be local adjustments to correspond with the actual environment.

Some complicating factors should next be considered in relation to the figures set out in Table 10. First, for low albite it is necessary to decide whether to treat an idealized fully ordered Al–Si distribution in which $Si_1(0)$ = Al, remaining tetrahedral sites = Si, or whether to assume that the actual distribution*

Table 10. *Bond strengths contributed by* Al^{+3}, Si^{+4} *and* Na^{+1} *to* O^{-2} *atoms in tetrahedral groups*

	Low albite				High albite	
Tetrahedron	(1)	(2)	(3)	(4)	(5)	(6)
$Si_1(0)$	7·83	7·71	8·02	7·90	8·17	8·14
$Si_1(m)$	8·08	8·18	8·03	8·13	8·00	8·00
$Si_2(0)$	8·08	8·18	7·93	8·03	8·00	7·93
$Si_2(m)$	8·00	7·93	8·00	7·93	7·83	7·93
	0·33	0·72	0·12	0·33	0·34	0·28

The columns (1) to (6) correspond to the following assumptions:—

(1) $Si_1(0)$ = Al, remainder = Si, Na coordinated by 6 oxygens $A(1)$, $A(1)$, $A(2)$, $B(0)$, $C(0)$, $D(0)$.
(2) $Si_1(0)$ = Al, remainder = Si, Na coordinated by 7 oxygens $A(1)$, $A(1)$, $A(2)$, $B(0)$, $C(0)$, $D(0)$ and $D(m)$.
(3) Actual Al–Si distribution; Na coordination as in (1).
(4) Actual Al–Si distribution; Na coordination as in (2).
(5) Random Al–Si distribution; either Na′ or Na″ occupied, or both at random, coordinated by 6 oxygen atoms.
(6) Random Al–Si distribution; Na′ and Na″ occupied at random, coordinated by 7 oxygen atoms.

The total deviation from balance $\Sigma|\Delta|$ is shown at the foot of each column.

* Pending the completion of the three-dimensional analysis, in order to take account of the apparent excess in total amount of Al the amount in each group is arbitrarily reduced by 10%, thus $Si_1(0)$ = 0·72, $Si_1(m)$ = 0, $Si_2(0)$ = 0·20, $Si_2(m)$ = 0·09, total 1·01.

described in Part I is typical of low albite. Secondly, in computing bond strengths contributed by Na^{+1} it is necessary to fix its coordination number: it may safely be assumed that any Na–O contact distance exceeding 3·2 Å may be ignored, but it is not obvious whether contacts ~ 3·0 Å, which raise the coordination number from 6 to 7 in both low albite and high albite (Tables 6 and 9), should also be ignored.* Thirdly, oxygen atom $A(2)$ needs special consideration; for in *all* the structures so far examined this atom makes the shortest contact with the cation—thus sanidine 2·70 Å, microcline 2·76 Å, orthoclase (subject to revision) 2·90 Å, for K^{+1} and low albite 2·36 Å, high albite 2·4 Å, for Na^{+1}; on the other hand in the ordered or partly ordered structures microcline, orthoclase (subject to confirmation) and low albite the atom $A(2)$ is bonded to atoms $Si_2(0)$ or $Si_2(m)$ which tend to contain little Al^{+3}. It might therefore be supposed that the short contact arises entirely from packing considerations and that no electrostatic bond is involved (cf. Bailey & Taylor, 1955, p. 630). This possibility has been examined in some detail for albite, and is found to lead to inconsistencies and difficulties more serious than any implicit in the treatment adopted in this paper, namely that electrostatic valence is to be reckoned from the coordination number of the cation irrespective of the variations in bond lengths from other ions to the coordinating anions, and that the very short contact to $A(2)$ is a direct consequence of its special situation relative to the cation cavity into which it tends to be thrust by the two tetrahedral groups of which it forms the common corner. Lastly, although in general the balance of charge on the individual oxygen atom should be studied, in albite it is convenient to consider the tetrahedral group as the unit, since the structural changes under discussion depend upon the Al–Si distribution within the tetrahedra. Tables 10 and 11 therefore contain only the figures for tetrahedral groups; none of the deductions based on these figures is contradicted if individual atoms are considered, though some are much less strikingly demonstrated.

Table 11. *Bond strengths contributed by* Al^{+3}, Si^{+4} *and* K^{+1} *to* O^{-2} *atoms in tetrahedral groups*

Tetrahedron	Microcline	Sanidine	'Orthoclase'
$Si_1(0)$	8·11	8·05	8·00
$Si_1(m)$	7·87		
$Si_2(0)$	8·00	7·94	8·00
$Si_2(m)$	8·08		
	0·32	0·22	0

Nine-coordination of K is assumed for all cases. For microcline and sanidine the observed Al–Si distributions are used in calculating bond strengths; for 'orthoclase' the figures correspond to the ideal case discussed in the text, § 3(*b*).

For both triclinic and monoclinic cases the total deviations $\Sigma|\Delta|$ are computed for corresponding numbers of tetrahedral groups (4).

A number of important conclusions may be drawn from the figures given in Table 10 for the charge balance for individual tetrahedral groups and for the total deviation from balance $\Sigma|\Delta|$ for the structure as a whole:

(*a*) For low albite, with either the actual Al–Si distribution or the idealized fully-ordered distribution, the charge balance is much better for 6-coordination than for 7-coordination of the Na atom. Henceforward we assume 6-coordination for this structure.

For high albite, with random Al–Si distribution, the deviation from balance slightly favours 7-coordination for Na. This is in accordance with expectation, but in any case it is not to be anticipated that in such a high-temperature disordered structure there will be either a well defined coordination-group or a very satisfactory charge balance.

(*b*) For low albite the actual Al–Si distribution corresponds to a much smaller deviation from balance than does the idealized fully-ordered distribution. This comparison between actual and fully-ordered Al–Si distributions is valid whether 6-coordination or 7-coordination is assumed for Na, but if we accept 6-coordination, as in (*a*) above, the discussion can be taken further, as follows. First, it is clear that the actual distribution (column (3) of Table 10) represents quite a good approximation to a perfect balance of charge, since $\Sigma|\Delta| = 0{\cdot}12$. Secondly, it is a simple calculation to show that perfect balance would be achieved for a distribution in which the site $Si_1(0)$ contains 0·75 Al, while each of the other sites $Si_1(m)$, $Si_2(0)$ and $Si_2(m)$ contains 0·08 Al. The accuracy of our two-dimensional analysis of the structure is not sufficient to enable us to decide whether the actual distribution shows a real departure from that predicted for a perfect charge-balance, and it would be premature to speculate on the possible bearing of our findings on the well-known variations in rate of transformation to high albite observed on heating low albites from different sources. It is, however, very significant that the actual distribution observed in the structure, which appears to differ appreciably from the fully-ordered distribution, corresponds to a much more stable system of electrostatic forces, and that (see (*d*) below) the general Al–Si distribution in low albite can be predicted from the charge distribution in high albite. Caution is necessary in thus developing the discussion of the importance of charge balance on the basis of a two-dimensional analysis (cf. significance tests, Table 8, and the corresponding text, Part I, § 3). It is therefore very satisfactory that the general ideas now under discussion are supported by evidence derived from the highly accurate three-dimensional analyses of potassium felspars (§ 3, below). We may then assert that there is considerable evidence

* Three-dimensional refinement may permit a definite decision on the coordination of the Na atom, but in our opinion this is unlikely where the cation coordination is so markedly irregular.

in favour of the view that the most stable structure for low albite is not one in which the Al–Si distribution is fully ordered, but one in which partial ordering results in the optimum distribution of electrostatic valence (or balance of charge).

(*c*) The greater stability of low albite in comparison with high albite can be correlated with the low value of $\Sigma|\Delta|$ computed for the actual Al–Si distribution and 6-coordination of Na, in low albite, compared with $\Sigma|\Delta|$ for high albite for either 6- or 7-coordination.

(*d*) It is possible to show why, starting with the random Al–Si distribution of high albite, as ordering proceeds Al tends to be concentrated* in group $Si_1(0)$. Columns (5) and (6) of Table 10 show that in high albite, assuming either 6- or 7-coordination for Na, the oxygen atoms of group $Si_1(0)$ alone receive appreciable excess total bond strength; hence as ordering begins Al will tend to enter $Si_1(0)$. Assuming 7-coordination for Na at this initial stage of the ordering process, column (6) shows that a corresponding movement of Si into sites $Si_2(0)$ and $Si_2(m)$ will begin; if 6-coordination is assumed instead, column (5) indicates a movement of Si only into $Si_2(m)$. As ordering proceeds, contact distances and bond strengths gradually change, and the above argument should not be assumed to apply to the later stages of ordering as it does to the initial onset of order; nevertheless the trend is correct, since the low albite actual distribution shows $Si_2(0) = 0{\cdot}20$ Al, $Si_2(m) = 0{\cdot}09$ Al. Nothing in the above argument shows why site $Si_1(m)$ should *lose* the 0·25 Al it contains in high albite, since the bonds to the four oxygens of that group total almost exactly 8, irrespective of the coordination assumed for Na. A more detailed consideration of the individual oxygen atoms, and of their bonds to Na, can be shown to lead to the prediction of a reduction in the Al content of $Si_1(m)$; the steps in the argument are not reproduced here, since it is difficult to be satisfied of their validity for such a complicated series of changes, but the total bond strength 8·03 achieved in the actual low albite structure, assuming 6-coordination for Na, shows that in the later stages of the ordering process the loss of Al from this site is essential for a satisfactory local balance of charge. Moreover, it must not be forgotten that factors other than balance of charge may influence the structure, and that in any case the exact proportions of Al in each site remain uncertain until the three-dimensional analysis is completed.

The excess bond strength received in high albite by the oxygen atoms of group $Si_1(0)$ is due to the fact that $A(1)$ makes contacts with two Na atoms, and is the only oxygen to do so; atom $A(1)$ also contributes to the group around $Si_1(m)$, but here its double contribution is offset by weaker-than-average contributions from other atoms. In other high-temperature felspar structures, however, this need not necessarily be so and we should then anticipate a tendency for concentration of Al into both groups $Si_1(0)$ and $Si_1(m)$; the application of this idea to the K felspars is discussed below.

The above treatment of ordering, based on charge distribution, appears to give a satisfactory account of the principal features observed. For, provided the most reasonable assumptions are made about the coordination of Na, a self-consistent model is obtained which accounts for the stability of low albite relative to high albite, for the initial tendency of Al^{+3} to be segregated into group $Si_1(0)$ as ordering begins, and for the observed retention of some Al^{+3} in a group or groups other than that in which it is chiefly concentrated.

De Vore (1956) is the only previous author to attempt to explain why ordering should occur, but we find it difficult to accept his treatment, if we have understood it correctly, since it appears to violate crystallographic symmetry requirements, and, moreover, takes no account of the cations Na, K or Ca.

3. Electrostatic charge distribution in microcline and sanidine

Discussion of charge distributions in these felspars is simplified because the large K^{+1} ion occupies fairly well-defined cavities, in both structures, with nine O^{-2} atoms at distances between 2·7 Å and 3·2 Å. Moreover, the groups $Si_1(0)$ and $Si_1(m)$ of triclinic microcline* are combined into a single group Si_1 in monoclinic sanidine, and similarly for Si_2, O_B, O_C, O_D; in such a monoclinic structure each atom O_B, O_C, O_D receives the same bond contribution (1·875) from the two tetrahedra to which it is common, irrespective of the Al–Si distribution. The bond strengths quoted in Table 11 for microcline and sanidine are computed from the figures given by Cole *et al.* (1949) and Bailey & Taylor (1955).

If we again accept balance of charge as a measure of stability, striking conclusions about the relationship between degree of Al–Si ordering and stability can be derived from the figures quoted in Table 11. It should be noted that this discussion rests entirely on accurate structure-analyses by three-dimensional methods.

(*a*) Microcline, the low-temperature partly ordered potassium felspar, is *less* stable than sanidine, the high-temperature form with random Al–Si distribution. Bailey & Taylor (1955) noted certain aspects of the poor charge balance in microcline, and concluded that geometrical packing considerations predominate over charge in controlling the coordination of K in that structure. While accepting the validity of this view of the importance of packing for the K-atom coordination, we are now able to offer a more complete discussion of the significance of the poor charge balance,

* For the actual low-albite distribution, and also for the fully ordered distribution, if such exists.

* In any comparison with albite it must not be forgotten that $Si_1(0)$, $Si_2(0)$, $B(0)$, $C(0)$, $D(0)$ of one structure correspond to $Si_1(m)$, $Si_2(m)$, $B(m)$, $C(m)$, $D(m)$ of the other.

in microcline, on the basis of our knowledge of the albite structures (§ 4, below).

(*b*) The structure of a K felspar with a perfect charge-balance, and hence presumably more stable than both sanidine and microcline, can be deduced in the following way. The argument already applied to the albites (§ 2(*d*)) indicates that when the random sanidine structure first begins to order, Al^{+3} tends to occupy tetrahedra of group Si_1, with a corresponding increase in the proportion of Si^{+4} in group Si_2. In the Na felspars the small Na^{+1} ion, occupying a cavity which is too big for it, contributes bonds only to 6 of the 9 oxygens enclosing the cavity, and the charge distribution is such that most of the Al^{+3} migrates to $Si_1(0)$, with changes in the unit-cell dimensions as ordering proceeds. With the K felspars, however, the large K^{+1} ion fully occupies its cavity and contributes bonds to all 9 enclosing oxygens; this being true for both sanidine and microcline, it follows that the redistribution of Al^{+3} and Si^{+4} as ordering proceeds should not necessarily require serious changes in the geometry of the structure nor, in particular, a change in symmetry. In this case, the stable low-temperature structure should remain monoclinic $C2/m$, and redistribution of Al^{+3} and Si^{+4} should proceed until the two types of tetrahedra Si_1 and Si_2 contain such proportions of Al^{+3} that balance of charge is achieved. With bonds $+\frac{1}{9}$ from K^{+1}, this corresponds to (0·36 Al+0·64 Si) in Si_1 and (0·14 Al+0·86 Si) in Si_2. It seems reasonable to conclude that the stable low-temperature form thus predicted may be represented by orthoclase, for which there is some evidence (Chao *et al.*, 1940) of ordering of the kind indicated, though definite proof of this proposed ordering scheme is still awaited (Cole *et al.*, 1949).

4. A possible origin for microcline

If the Al–Si ordering process in sanidine produces orthoclase as the stable structure, it is necessary to show under what conditions ordering results instead in the unstable microcline structure. In particular, it should be possible to suggest why in microcline one group $Si_1(m)$ should be enriched in Al^{+3}, with the associated change of symmetry from monoclinic to triclinic. It is proposed that the microcline type of ordering arises from the influence of sodium atoms, in the following way.

Microclines frequently occur in albitized pegmatite, and microcline perthites (including micro- and cryptoperthites) are very common. Furthermore, heating experiments such as those of Spencer (1937) have shown that microperthites are readily homogenized at relatively low temperatures (350–750° C.), this change being supposed to correspond to disordering of the K^{+1} and Na^{+1} ions throughout the available cavities without any change in the Al–Si distribution which would require the much more severe heat-treatments resulting in sanidinization. Let us assume that the converse process operates similarly, so that the K–Na distribution remains random throughout the range of high temperatures in which Al–Si ordering takes place as temperature falls. Then, if the alkali atoms are mostly K, the Al–Si ordering should approximate to that for the partially ordered monoclinic orthoclase described above, whereas if Na predominates the Al–Si ordering should be like that of low albite, and for more nearly equal proportions of K and Na an ordered arrangement intermediate between the two would be expected. Table 12 shows that this is in agreement

Table 12. *Comparison of* Al–Si *distributions in low-temperature felspars*

Tetrahedral group	Low albite	Microcline	'Orthoclase'
$Si_1(0)$	0·72	0·56	0·36
$Si_1(m)$	0	0·25	0·36
$Si_2(0)$	0·20	0·08	0·14
$Si_2(m)$	0·09	0·07	0·14

The figures show the proportion of Al^{+3} in each tetrahedron. For low albite the figures are those given in the footnote to § 2 above, for (monoclinic) 'orthoclase' the figures are those in § 3(*b*), and for microcline those of Bailey & Taylor (1955). The numbering of the four groups is that appropriate to low albite.

with observation, at least in general terms; it must not be forgotten that the figures for Al-content in low albite are subject to amendment (probably small) when the results of three-dimensional syntheses become available. On passing to lower temperatures the perthitic structure appears as separate K-rich and Na-rich regions, but it is no longer possible for any serious change in Al–Si ordering to take place; the most that can happen as the tetrahedron framework in each of these regions seeks to accommodate either predominantly K ions or predominantly Na ions is a small reorientation of the tetrahedra. In such a structure the K-rich component of a perthitic microcline will show unbalance of charge since the large K^{+1} ion is within an Al–Si distribution appropriate to the average K–Na cation of the high-temperature structure. (Similarly, the Na-rich component would show unbalance, for the same reason.)

On this view, the presence of sodium during cooling is essential to the formation of a microcline; whether a 'maximum microcline' corresponds to a higher proportion of sodium is not certain, though this seems probable when the figures in Table 12 are considered in relation to the opinion of Bailey & Taylor (1955, p. 630) that in a maximum microcline all or most of the Al^{+3} is concentrated in one tetrahedron. This argument provides at least a partial explanation for the contrast between the abundance of intermediate microclines and the rarity of albites intermediate in structure between low albite and high albite. Its development for a wider treatment of the origin of the various alkali felspars will be considered elsewhere, but its potential importance for petrological purposes is obvious.

Thus the treatment which offered a consistent model for the albites also provides a reasonable account of the relationship between Al–Si order and stability in the potassium felspars, and gives significance to the distinction between triclinic microcline and monoclinic sanidine and orthoclase.

5. Conclusion

It is necessary to proceed with caution in deriving generalizations from structures in some of which the refinement is restricted to that obtained by two-dimensional methods, and in basing arguments about structural stability on discussions of electrostatic charge balance when it is not certain that the interatomic forces are purely ionic, although it is frequently found that this procedure is satisfactory even when it is known that non-ionic forces are involved.

Nevertheless, such considerations lead to a consistent explanation of the relative stability of high albite and low albite, and of the nature of the ordering process in detail, and suggest that the more accurate structure to be obtained from a three-dimensional analysis will suggest reasons for a number of hitherto unexplained experimental observations on the high-low transition.

In addition, it seems highly probable that an enhanced degree of Al–Si ordering need not necessarily be associated with greater stability in the potassium felspars; and that there is not one series increasing continuously in stability from sanidine to maximum microcline, but two series of which one begins with sanidine and runs to a partially-ordered orthoclase as both degree of Al–Si order and stability increase, while the other begins with a highly-ordered maximum microcline and also runs to the same monoclinic orthoclase but with stability increasing as order decreases.

It is also very probable that complete concentration of all the Al^{+3} into one tetrahedral site is not achieved even in the most highly-ordered alkali felspars, with the doubtful possible exception of a maximum microcline.

The ideas developed in the preceding discussion are not regarded as proved with complete certainty but they do have the merit that they are based on the measurements available and that they may provide a satisfactory explanation, for example, for the origin of microclines. Their application to other petrological aspects of the felspar problem is under consideration. They are opposed to some aspects of the structural models advanced by Goldsmith & Laves (1954). They may be confirmed, or the need for their modification may be demonstrated, when the three-dimensional refinement of the albite structures is completed and when the results of a revision of the orthoclase structure become available shortly in the Laboratory of one of the authors (W. H. T.).

References

Bailey, S. W., Ferguson, R. B. & Taylor, W. H. (1951). *Miner. Mag.* **29**, 759.

Bailey, S. W. & Taylor, W. H. (1955). *Acta Cryst.* **8**, 621.

Barth, T. F. W. (1934). *Amer. J. Sci.* **27**, 273.

Baskin, Y. (1956). *J. Geol.* **64**, 132.

Booth, A. D. (1948). *Fourier Technique in X-ray Organic Structure Analysis.* Cambridge: University Press.

Bragg, W. L. & West, J. (1928). *Z. Kristallogr.* **69**, 118.

Chao, S. H., Hargreaves, A. & Taylor, W. H. (1940). *Miner. Mag.* **25**, 498.

Cochran, W. (1948). *J. Sci. Instrum.* **25**, 253.

Cochran, W. (1951). *Acta Cryst.* **4**, 81.

Cole, W. F., Sörum, H. & Kennard, O. (1949). *Acta Cryst.* **2**, 280.

Cole, W. F., Sörum, H. & Taylor, W. H. (1951). *Acta Cryst.* **4**, 20.

Cruickshank, D. W. J. (1949). *Acta Cryst.* **2**, 65.

De Vore, G. W. (1956). *J. Geol.* **64**, 31.

Emmons, R. C. [Editor] (1953). *Geol. Soc. Amer. Mem.* **52**.

Goldsmith, J. R. & Laves, F. (1954). *Geochim. Cosmoch. Acta.* **6**, 100.

Howells, E. R., Phillips, D. C. & Rogers, D. (1950). *Acta Cryst.* **3**, 210.

Laves, F. (1951). *J. Geol.* **59**, 510.

Laves, F. (1952). *J. Geol.* **60**, 549.

Laves, F. & Chaisson, U. (1950). *J. Geol.* **58**, 584.

Lipson, H. & Cochran, W. (1953). *The Determination of Crystal Structures.* London: Bell.

Megaw, H. D. (1956). *Acta Cryst.* **9**, 56.

Smith, J. V. (1954). *Acta Cryst.* **7**, 479.

Spencer, E. (1937). *Miner. Mag.* **24**, 453.

Taylor, W. H. (1933). *Z. Kristallogr.* **85**, 425.

Taylor, W. H., Darbyshire, J. A. & Strunz, H. (1934). *Z. Kristallogr.* **87**, 464.

Tuttle, O. F. & Bowen, N. L. (1950). *J. Geol.* **58**, 572.

Weisz, O., Cochran, W. & Cole, W. F. (1948). *Acta Cryst.* **1**, 83.

Weisz, O. & Cole, W. F. (1948). *J. Sci. Instrum.* **25**, 213.